GEOCHRONOLOGY and THERMOCHRONOLOGY

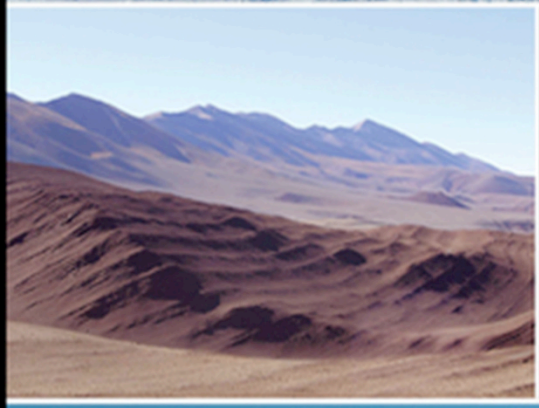

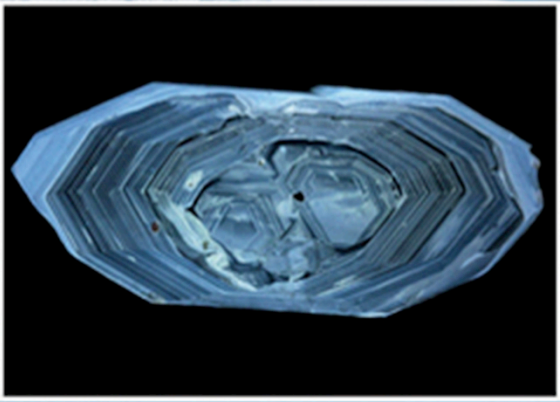

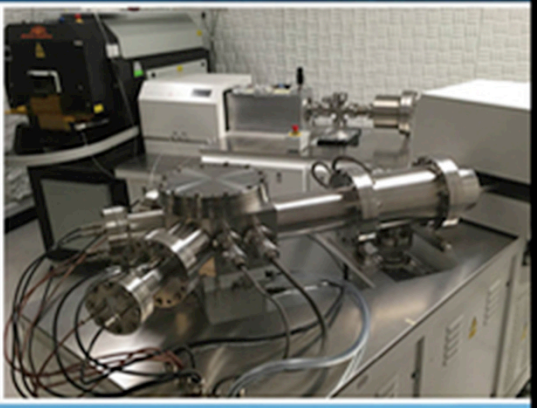

Peter W. Reiners, Richard W. Carlson, Paul R. Renne, Kari M. Cooper, Darryl E. Granger, Noah M. McLean, and Blair Schoene

AGU American Geophysical Union

WILEY

Geochronology and Thermochronology

Geochronology and Thermochronology

Peter W. Reiners
University of Arizona
Tucson, AZ, USA

Richard W. Carlson
Carnegie Institution for Science
Washington, DC, USA

Paul R. Renne
Berkeley Geochronology Center
and
University of California
Berkeley, CA, USA

Kari M. Cooper
University of California, Davis
Davis, CA, USA

Darryl E. Granger
Purdue University
West Lafayette, IN, USA

Noah M. McLean
University of Kansas
Lawrence, KS, USA

Blair Schoene
Princeton University
Princeton, NJ, USA

AGU
American Geophysical Union

WILEY

This edition first published 2018

Registered Office(s)

John Wiley & Sons, Inc., 111 River Street, Hoboken, NJ 07030, USA

John Wiley & Sons Ltd, The Atrium, Southern Gate, Chichester, West Sussex, PO19 8SQ, UK

Editorial Office

9600 Garsington Road, Oxford, OX4 2DQ, UK

The Atrium, Southern Gate, Chichester, West Sussex, PO19 8SQ, UK
111 River Street, Hoboken, NJ 07030, USA

For details of our global editorial offices, customer services, and more information about how to apply for permission to reuse the copyright material in this book please see our website at www.wiley.com/wiley-blackwell.

Library of Congress Cataloging-in-Publication data is available.

ISBN: 978-1-118-45585-2 (cloth)
978-1-118-45578-4 (paper)

A catalogue record for this book is available from the British Library.

Cover image: (Front cover top) Photo by Sonia Esperance; (Center image) Photo by George Gehreis; (Front cover left and right images; Back cover image) Photos by Peter W. Reiners

Cover design by Wiley

Set in 9/12pt Galliard by SPi Global, Pondicherry, India

Printed in the United States of America

10 9 8 7 6 5 4 3 2 1

Contents

Preface

Geochronology, including thermochronology, is an essential component of practically all modern Earth and planetary science and provides fundamental information for many other areas, including archeology, marine sciences, and ecology. Geochronology establishes the timing of critical events ranging from the age of the Earth to stratigraphic boundaries, and it provides unique constraints on the pace and dynamics of processes ranging from condensation of the solar nebula to planetary differentiation to surface exposure to biologic evolution. Given that Earth and planetary scientists commonly seek to understand relationships between events or phenomena for which physical evidence is incomplete or ambiguous, establishing temporal relationships through geochronology often provides a substantial basis for causality arguments.

Although the concept of geochronology has existed for millennia, and the particular name has been around since 1893, most scientists would probably agree that the modern practice or discipline is based on application of radioisotopic (or cosmogenic) systems in natural materials, which has existed for only a little more than a century (or less). Even into the 20th century, the geologic timescale floated freely in time. Geologists had established sequences of evolutionary and orogenic events in the rock record, but numerical estimates ranged widely, more so further back in geologic history. Without precise dates, only poorly constrained arguments could be made about the relative durations and the time separating major events in the geologic record. Likewise, prior to radioisotopic methods, the best available estimates for the age of the Earth (and solar system) disagreed by several orders of magnitude. The rather sudden recognition of nuclear structure and radioactive decay around the beginning of the 20th century, changed Earth and planetary science fundamentally. The very first radioisotopic dates measured increased the previously deduced minimum age of the Earth by about an order of magnitude, and subsequent work, less than 100 years ago, increased it by another factor of ten.

Although the numerical age of the Earth and the temporal anchoring of the geologic timescale are of immense practical (as well as philosophical and fundamental) value, these were only a start to the revolution that radioisotopic geochronology imparted to Earth and planetary sciences. Geochronology continues to be essential in the way it was originally used, to establish formation ages of rocks, but has also evolved into a broad array of methods and approaches for providing temporal constraints on natural phenomena ranging from the pacing of orbital oscillations, rates of erosion and paleotopographic change, subsurface fluid fluxes, timescales of lithospheric recycling to the deep mantle, periodicity of continental growth, collisions in the asteroid main belt, and much more. Modern geochronology is about more than dating events—it is also about using rigorous, quantitative, and innovative approaches to measuring rates, fluxes, and timescales, and using temporal constraints to understand the processes driving natural phenomena.

Our book is intended to provide both an introduction and reference for users and innovators in geochronology. Because it is a dynamic field, many aspects of geochronology change quickly, from the atomic-scale understanding of radioisotopic decay, experimental investigations and kinetic calibrations of thermal (and other) sensitivities to daughter product retention, analytical measurement techniques, mathematical modeling and interpretational approaches, and the types of geologic or planetary questions on which applications focus. We have done our best, in the chapters of this book, to provide modern perspectives on the current state-of-the art in most of the principal areas of geochronology, while recognizing that they are changing rapidly. We intend for students and scientists to use the chapters in this book as a foundation for understanding each of the methods we cover, and for illuminating directions that we think will be important in the near future. Users of this edition of this book may wish to complement the chapters with emerging references and reviews to provide valuable perspectives on the fields and topics, as well as opportunities for important questions and problems in the near future. We have attempted to provide sufficient references to rapidly evolving topics that will enable readers to pursue future developments via citation strings in bibliometric databases.

This book attempts to present the state-of-the-art on most of the most important geochronologic methods, emphasizing fundamentals and systematics, historical perspective, analytical methods, data interpretation, and some applications chosen from the literature. The presentation is designed to be useful to students in graduate courses or to upper-level undergraduates with a solid background in mathematics, geochemistry, and geology. Although this book will be useful as a reference to users, we cannot make claims to encyclopedic coverage of all these topics. Indeed actual encyclopedias of dating techniques are available elsewhere. In addition, this book is different from the several others that do an excellent job of describing geochronology as a subfield or application of isotope geochemistry. We cannot supplant the comprehensive utility of isotope geology books, but we aim to complement them by expanding on those parts of isotope geochemistry that are concerned with dates and rates and insights into Earth and planetary science that come from temporal perspectives. We have attempted to present the fundamentals,

perspectives, and opportunities in modern geochronology together in a way that we hope will inspire further innovation and creative technique development and applications.

We acknowledge helpful reviews and advice from several colleagues, particularly Rebecca Flowers and Peter Zeitler, who provided helpful feedback on the entire book. We are also grateful to reviews and advice from Willy Guenthner, Frederic Herman, Richard Ketcham, Georgina King, Larry Nittler, Stuart Thomson, Jibamitra Ganguly, and Doug Walker, and editorial assistance from Matt Dettinger, Diana Gutierrez, and especially Erin Abel. We also gratefully acknowledge the strong and vibrant community of geochronologists and thermochronologists in Earth and planetary science today, who may not always agree but who inspire our desire to contribute to the geochronologic conversation and wield the power of radioisotopic dating to gain and share real insights to nature.

Peter W. Reiners
Richard W. Carlson
Paul R. Renne
Kari M. Cooper
Darryl E. Granger
Noah M. McLean
Blair Schoene

CHAPTER 1

Introduction

Occasionally debates arise and hands are wrung about what parts of a scientific discipline really distinguish it from others. Geoscientists often find themselves trying to define the unique perspectives or essential skills at the heart of their field as if failure to properly indoctrinate students in them might put the entire profession at risk. Without commenting on the wisdom of such disciplinary exceptionalism, a reasonable person asked to engage in it could, after some thought, suggest that if there is something distinctive about Earth science, it might have something to do with time. Naturalistic thinking about the evolution and workings of the Earth have been around for centuries if not millennia, and considerations of time at scales far surpassing human experience are a central and obligatory part of any serious endeavor in this area. The facility to deal easily with enormous timescales is such an ingrained part of Earth and planetary science that occasional meditative realizations of even the most hardened scientists are sometimes required to remind them that our ability to envision geologic time accurately and precisely has been in some ways hard won. Before quantitative measurements were available of the durations of time separating events of the past from the present, and of the rates of geologic processes, practically all attempts to understand Earth were, to paraphrase a key historical figure in geochronology (Lord Kelvin), meagre and of a most unsatisfactory kind. Quantitative geochronology as a concept, and especially radioisotopic geochronology as a field in and of itself, revolutionized our understanding of the Earth and planets. More importantly, geochronology continues to be one of, if not the most, important foundation and means of exploration in modern geoscience.

The tools and applications of geochronology find use in a variety of fields besides Earth and planetary science, including archeology, evolutionary ecology, and environmental studies. But the impact of geochronology on Earth science was fundamentally transformative. For one thing, it laid out the boundary conditions for reconstructing the history of the planet and quantitative understanding of the significance of ongoing physical processes like erosion, sedimentation, magmatism, and deformation. It also established, for the first time, a realistic temporal context of existence—not just of life as we know it, but for the recognizable planetary environment that hosts life. This is because the timescales of Earth history and Earth processes (including biotic evolution at that scale) require a fundamentally different temporal perspective than human experience (much less historical records) can offer. While some important geologic and evolutionary processes happen over very short timescales and require chronometers with commensurate sensitivity, many of the most challenging and important observations we make about the Earth reflect processes that occur either very slowly or very rarely, relative to the perspective of humans as individuals, civilizations, or even species. Modern radioisotopic techniques span vast timescales from seconds to billions of years, finding application in problems ranging from the age and pace of individual volcanic eruptions to condensation of the solar nebula and ongoing planetary accretion. The transformative power of geochronology comes from its capacity to expand our understanding beyond the reach of the pathetically short timescales of intuitive human or social perspectives.

1.1 GEO AND CHRONOLOGIES

Extending the timescale of our understanding does not mean just establishing a chronology of events that occurred earlier than historical records or generational folklore allow. It goes without saying that establishing pre-historical records of changes on and in Earth and other planets is practically useful: knowing when a volcano erupted or a nearby fault last ruptured or the age of an extinction or diversification event may be important. Establishing historical chronologies of tectonic events is clearly necessary for practical purposes. But a list of dates or sequence of regional events is of limited value in and of itself, and does little to represent geochronology as way of

Geochronology and Thermochronology, First Edition. Peter W. Reiners, Richard W. Carlson, Paul R. Renne, Kari M. Cooper, Darryl E. Granger, Noah M. McLean, and Blair Schoene.

exploring how the planet works using time as an organizing principle or mode of inquiry.

For one thing, there is the question of how to define an event. At one level the question of the age of the Earth is simple, and has been the focus of countless studies since human curiosity began. Modern perspectives on the problem however, shifted years ago from simplistic numerical answers of around 4.56 Ga, to more sophisticated ones that raise issues of how to assign a single age to a protracted evolutionary process complicated by questions of the initial uniformity of and chemical fractionation in the solar nebula, and timescales of accretion, mass loss, and differentiation. Many other questions in Earth and planetary science have evolved similarly as understanding deepened. Continuing efforts to understand the geologic record are no longer satisfied with just knowing "the age" of a particular event such as the Permo-Triassic boundary, the Paleocene–Eocene Thermal Maximum (PETM), or meltwater pulse 1A, but now we need to know the duration, pace, and number of perturbations composing an event, and the detailed sequence and timing of resulting effects. Geochronology has been central to all of these as not only the intended accuracy and precision, but also the essence of the question, changed. Geochronology shows that "events" are not only finite and messy, but manifestations of more interesting phenomena in themselves.

Also, while some scientists see geochronology as a useful tool for addressing pre-defined geologic problems, using geochronology is not the same thing as doing it. The power of geochronology arises from innovative approaches. There is no single template for this, but one could make an argument for at least two types of creative geochronology. The first is adapting new geochemical, physical, or analytical insight or technology to addressing suitable geologic problems. Fission-track dating was developed after methods for observing cosmic ray tracks in insulators were extended to tracks produced by natural radiation sources *in situ* [*Fleischer and Price,* 1964]. Inductively coupled plasma mass spectrometry and its pairing with laser ablation sample introduction both changed isotope geochemistry and geochronology in key ways [e.g., *Halliday et al.,* 1998; *Lee and Halliday,* 1995; *Kosler et al.,* 2008]. K–Ar dating was adapted into one of the most precise and powerful geochronological techniques ever developed ($^{40}Ar/^{39}Ar$ dating) using fast neutron irradiation to create proxies of parent nuclides of the same element and chemical behavior as the daughter nuclides [*Merrihue and Turner*, 1966]. And of course the first radioisotopic date itself was calculated as a marginalia to a nuclear physics study much more concerned with "radioactive transmutations" than with determining the age of anything [*Rutherford*, 1906].

Second, and as is true in many other fields, some impactful advances in geochronology have come not from deliberate engineering but more as refusals to ignore complications. Solutions to such problems often hold potential for illuminating unknown unknowns, which may then be trained to address previously unsolvable problems. When a particular technique appears to "not work" for answering the question originally posed, it may be time to ask why the answer is unexpected and what can be learned from it by reframing the question. Thermochronology, for example, owes a great deal of its modern utility to this sort of lemons-to-lemonade evolution, as the diffusive loss of daughter products was initially considered a debilitating limitation of noble-gas-based techniques [e.g., *Strutt*, 1906] but is now recognized as its defining strength, as increasingly complex as it appears to be [e.g., *Shuster et al.*, 2006; *Guenthner et al.*, 2013].

This is all to say that geochronology is not just a "tool" serving other fields, but is a field unto itself, and one that originates the new ideas and approaches that allow for advances in the areas to which it is applied. Geochronology generates the innovative ways to use nuclear physics and geochemistry to understand natural processes, often by using initially problematic aspects of these systems, and adapting them to questions that initially may not have been asked. It was not until long after we started wondering about the age of the Earth that we started to appreciate questions about the duration of events, stratigraphic boundaries, and diachroneity. And it was not until we developed quantitative tools (serendipitously, in many cases) for measuring dates and rates in new ways that we began to realize the value of understanding many more nuanced time-related problems, like rates of erosion, sedimentation, crystallization, or groundwater flow, the degree to which these processes are steady or episodic, and the scale at which these questions even make sense.

There is no denying geochronology's utility for addressing some of the most fundamental and, in many cases, simple questions in Earth and planetary science. This is true in both a historical sense, as geochronology provided key foundations for geoscience progress over the century, as well as in a continuing sense, as it continues to provide simple formation and cooling ages essential to many geologic studies. So it is reasonable to begin here with a review of the history of geochronology in the context of its original mothers of its necessity: the age of the Earth and, soon thereafter, ages of stratigraphic boundaries. The last part of this chapter then returns to the broader topic of geochronology—the discipline and its objectives and significance—with the hope that the perspective of the historical review drives these home.

1.2 THE AGES OF THE AGE OF THE EARTH

It is impossible to know when humans or perhaps their predecessors first started posing questions about the age of the Earth, but it seems likely that it has been a central focus of human contemplation for millennia. The scope and context of the question has likely changed, and in fact continues to evolve as our resolution of the early days of the solar system improves [*Bouvier and Wadhwa*, 2010; *Brennecka et al.*, 2010]. Ancient Greek and Hindu philosophies explained the age of the "world" in terms of infinite or cyclical ages, the latter punctuated by revolutions of destruction and rebirth, a theme that may originate from the rise and fall of human civilizations, but which may also have

been inferred by observant early naturalists from the rock record's evidence for episodes of upheaval and deformation followed by quiescence and slow accumulation.

Propositions for noncyclical and finite ages have also been around since ancient times. Early estimates for a finite age of the Earth (or "world"), which typically have more religious than philosophical origins, tended to converge on timescales in the thousands of years. These included Zoroasters 17th century BCE estimate of 12,000 years, and numerous estimates based on scrutiny of details in the Christian bible. No less than eight well established bible-based estimates for the age of the Earth are known from 169 and 1650 CE, bookended by the Syrian saint Theophilus of Antioch and the famous "scholarship" of James Ussher. All of these invoke ages between 5000 and 9000 years, and all but one are within a narrower range of 5500–7500 years.

The convergence of many "world" chronologies in the range of a few thousand years ago to millennial timescales is an interesting target of speculation. The 1000-year timescales may arise from being just beyond the reach of multigenerational memory of oral histories, but not so far as to seem unreasonable or intuitively incomprehensible. This timescale also is commensurate with the rise and fall of some of the most persistent political empires and cultural dynasties, as well as the timescale of the development of recorded human history. In any case, the eventual recognition that the age of the Earth was not infinite but is actually a million times greater than a few thousand years represented a slow-moving but important change in human perception. That the planet has a deep history of such immensity that it practically challenges our ability to conceive of it, and that it predates humans' presence by more than three orders of magnitude, has been called the fourth great revolution in human cognition [*Rudwick*, 2014].

Although not scientific in modern senses, some scholars consider early attempts to estimate the age of the Earth using biblical records historically important. Many of these essentially counted the number of human generations since the birth of Abraham. Like other pre-Enlightenment scholars who mixed religious and scientific approaches, Johannes Kepler combined biblical accounts with astronomy to arrive at very similar ~6000 ka ages for the Earth as late as the early 17th century. One of the best known of these biblically based, but astronomically laced, deductions is that of the Bishop James Ussher, who in the middle of the 17th century presented the results of his scholarship proposing the beginning of the Earth to be 22 October 4004 BCE. The "9:00 a.m." often associated with Ussher's estimate actually comes from a separate but similar account from a contemporary scholar, John Lightfoot, who put the beginning at the autumnal equinox of 3928 BCE. Incidentally, these results are a good example of the difference between accuracy and precision: Lightfoot's extremely precise time-of-day estimate was a full 76 years younger than Ussher's, and both were obviously lacking much more in the way of accuracy. Readers interested in these early examples are directed to more thorough accounts in G. Brent Dalrymple's "*The Age of the Earth*" [1994] and references therein.

Some historians of the evolution of thinking about the age of the Earth have suggested that early Christian accounts represent respectable nascent attempts to at least take the question seriously and start to frame the problem and possible solutions to it in an analytical and evidentiary way, even if the basis of the evidence was not scientific. Historian Martin Rudwick, in "*Earth's Deep History*" [2014], for example, calls Ussher's work "rigorous," and claims that it does not deserve the ridicule it commonly endures. It may indeed have been a rigorous examination of a document; less clear is the rigor of the documentation of the generations, much less their initiation as a proxy for the birth of the planet. But it may be true that Ussher's studies (and those of a few others) were not exactly sycophantic religious repetition then, but actually somewhat at odds with prevailing eternalism, the idea that the Earth has existed literally forever, at least insofar as humans are capable of understanding, and which to many seemed more reasonable and potentially reconcilable with biblical teachings. Thus Ussher's work and that of others might be considered the beginning of attempts to have a serious think about how old the Earth *could* be, using the scholarly resources available at the time. Rudwick argues that these efforts, while based largely on scripture, are continuous with later scientific attempts, which arose from the same progressive effort to understand the world. To that extent, it may be true that early studies by Ussher and others are distinguished from those of modern creationists (including proponents of intelligent design), whose absurdities are not honest attempts to comprehend anything and do not represent even primitive roots of any kind of legitimate understanding.

But before Ussher gets too much credit, his analysis was based on a religious text that represented the political, economic, and cultural authority of the time, so he probably did not lose sleep worrying whether his "rigorous" scholarship might put him in very real danger at the hands of the Christian power structure, as Galileo and others had only a few years earlier. So although Ussher's work may be detailed and arguably historically important, and may represent an early attempt to challenge the idea of equally nonscientific "eternalism," it does not rank with intellectually honest and courageous work of secular pioneers of the time who risked, and in many cases paid, the price of censure or far worse for crossing church authorities. In any case, the real challenge to human thinking (and, as it turns out, the scientific truth) though, is far different from both the relatively simple perspectives that either the Earth is eternal or its history is basically conceivable in terms of human generations. The far stranger truth is that the Earth is incredibly old, but has a finite age. Indeed it is the fact that it was born a knowable number of years ago in a relatively short period of time which we can know with somewhat startling precision that raises even more questions.

Although some 17th century scholarship on the age of the Earth mixed astronomical observations or theory with "textual" constraints, the Enlightenment brought new ideas about rates of

natural processes and actual geologic observations to bear on the question. One important figure in this vein was French diplomat and amateur naturalist Benoit de Maillet. In the early 17th century he constructed a theory for the age of the Earth told through an ingenious parable designed to avoid directly antagonizing the powerful Christian church (undermining Rudwick's claims that the Christian theocracy was no barrier to free thought at the time). Speaking through his fictional Indian philosopher Telliamed (his surname backwards), he combined measurements of rates of regional sea level decline with the height of high mountains and a Cartesian assumption (common at the time) that the earliest Earth was completely covered by ocean and that water was continuously lost through Descartes' mysterious vortices. This led him to the conclusion that the highest terrain must have been covered in water more than two billion years ago, providing a minimum age for the age of the Earth. Although the initial condition and steady decline of sea level is clearly absurd, de Maillet's analysis deserves credit for combining geologic observations and uniformitarian arguments to derive an estimated duration and therefore age constraint.

Other notable 18th and early 19th century attempts to constrain the age of the Earth also followed the general approach of combining a process occurring at an assumed rate with an initial condition of some sort. A popular one was cooling of an initially molten or at least extremely hot Earth. Although as far as we know, Isaac Newton did not directly wade into the debate over the age of the Earth, in the late 17th century he calculated cooling times for planetary bodies and speculated about cooling durations of comets that passed close to the Sun. His contemporary Gottfried Leibniz also speculated about the origins of topography as resulting from differential contraction during cooling of the initially molten Earth. Neither Newton nor Leibniz used cooling timescales to actually estimate ages of planetary or solar bodies, perhaps because they recognized the potential complexities involved, this of course became a popular sport a few hundred years later, in the late 19th century. But long before the famous calculations of physicist William Thomson helped earn him the title of Lord Kelvin, similar experiments and calculations of the provocative natural historian George-Louis LeClerc helped earn him the title Comte de Buffon.

Buffon wrote his major work on the origin of the Earth, "*Époques de la Nature*," in 1778. By this time, advances in natural history had established evidence that Earth history was not static or eternal, but that the planet had changed progressively over time. This included recognition, attributed at least partially to Nicolas Steno, that sedimentary rocks lower in stratigraphic sequences, and hence older, contained macroscopic fossils that appeared to be morphologically simpler than the rocks above them. And in fact the oldest rocks contained no identifiable fossils at all. Progressive change over time, rather than strict steady-state concepts of Earth history, was an important basis of Buffon's (and others') thinking. Although he recognized uniformitarian principles, for example as represented in erosion and deposition, he did not extend these to a simple eternalist vision of the Earth as many other contemporary thinkers, including the purported founder of modern geology, James Hutton, whose strong Christian convictions pervaded his avoidance of questions on the age of the planet, as in "[the Earth shows] no vestige of a beginning, no prospect of an end."

In fact, Buffon's publication "*Nature's Epochs*" ventured to estimate both ends of Earth's history that Hutton said were unknowable. Although many aspects of Buffon's analysis were highly speculative, such as the origin of the Earth (and other planets) by impact of a large comet with the Sun, his work was some of the first to apply basic physics and experiments to the question. Recognizing, as many did by that time, that temperatures beneath the Earth's surface generally increase with depth, Buffon combined this with the then well-accepted idea that the primeval Earth was entirely molten, and set about to experimentally determine the duration of time required to cool an Earth-size body to present surface temperatures. Using cooling times of cast iron balls of varying size at initially high temperatures, he extrapolated his experimental results to determine a minimum age for the Earth on the order of 100 ka. Buffon considered this likely far too low, for reasons that are not entirely obvious but probably related to his recognition that stratigraphic thicknesses required longer timescales if achieved by typical erosion and deposition rates, an apparent problem that was to plague the issue of the age of the Earth for the next ~150 years.

Buffon's cooling timescale experiments, which were built on those of Newton, Liebniz, and others before him, also foreshadowed some of the well-recognized thinking of one of the 19th century's most celebrated scientists, William Thomson, later named Lord Kelvin, whose influence and subsequent arguments have been documented well by *Burchfield* [1975], *Stacey* [2000], and in many other places. Beginning with the same convenient initial condition that the Earth began as a uniformly very hot sphere that cooled gradually with time, simple thermal diffusion arguments led to the basic conclusion that the current surface temperature and near-surface geothermal gradient required something on the order of 100 Ma [*Kelvin*, 1863], a number that he later revised to 20 Ma. Although it was widely recognized as heuristic, and well known that any internal advection would change the result to some degree, this estimate stood as the most reasonable and definitely the most authoritative estimate for more many decades. It also put most geologists (and the few evolutionary biologists of the time), who felt that the Earth must be far older based on observed timescales of ongoing processes, at odds with much of the scientific establishment for the next several decades.

The common account of the reason Kelvin's estimate was so far off is that it came from failure to account for the contribution of radioactive decay to Earth's internal heat. In reality this additional heat is not very significant to the basic result, and its incorporation would not have changed things significantly. The true explanation of the erroneous result is its failure to incorporate the much more effective advective, instead of conductive, transport of heat from throughout Earth's interior to the thin crustal

layer where the thermal gradient used in Kelvin's calculations was measured. A far more influential reason that most of the scientific community chose to accept the physicists' estimates over the longer views of geologists came from Kelvin's work on the estimated age of the Sun. Using similar approaches, Kelvin had argued that the Sun could only contain enough heat after initial formation to remain as hot as it now is for no more than about 20 Ma. Assuming that the Earth itself was unlikely to predate the Sun, this placed a strong upper bound on the age of the Earth. Even the discovery of radioactive decay of naturally occurring nuclides near the turn of the century would not change the basics of this argument, as nuclear fusion was not recognized until the 1920s or 1930s, extending the debate and undercurrent of animosity between geologists and physics for several more decades.

Among the many geologists resistant to Kelvin's constraints was then University of Chicago professor Thomas Crowder Chamberlin. Also recognized for proposing that changing CO_2 concentrations in the atmosphere may be responsible for climate change, he suggested that Kelvin's timescale was too short to reconcile with geologic evidence and that there must be another source of heat within the Earth. From this debate comes one of his well cited quotations:

> "*The fascinating impressiveness of rigorous mathematical analysis, with its atmosphere of precision and elegance, should not blind us to the defects of the premise that condition the process.*" [*Chamberlin*, 1899]

Ironically, it would be the physicists again, including a Kiwi by the name of Ernest Rutherford known for the quote, "*All science is physics or stamp collecting,*" who would all underscore Chamberlin's quote by not only helping find the additional heat source but also creating the means for accurate and increasingly precise quantification of the real age of the Earth.

Several other approaches to estimate the age of the Earth were also taken near the end of the 19th century and beginning of the 20th. One of the more productive, at least in terms of numbers of papers, was based on ocean salinity. As described by *Dalrymple* [1994] the "salt accumulation clock" method was first proposed by Edmund Halley (of comet fame), who reasoned as early as 1715 that comparing the total salt content of the ocean to the amount delivered by rivers could provide an estimate of the age of the ocean and, to the extent that the Earth has always had an ocean (and that it began as freshwater…), the Earth itself. Between 1876 and 1909 T. Mellard Reade and later John Joly, as well as others, picked up the approach and derived estimates falling between 25 and 150 Ma, with later estimates tending to inch upwards. The fact that the approach yielded answers converging on something similar to Kelvin's calculation based on heat flow probably aided its apparent legitimacy. But as we recognize now, even if delivery rates of ions to the ocean from rivers (and groundwater, as we now also know is an important source) were to stay constant with time, the ratio of the total amount of any ion in the oceans to this rate does not necessarily produce a time that corresponds to an initial concentration of zero. Analogous to the problem of coupled production and diffusion in open-system thermochronometers, the ratio of current inventory to current rate of accumulation does not account for fluctuations in both through time. In addition to the likelihood that the ocean was not born fresh, it is also subject to loss of its dissolved load at a rate that may vary itself over time. The apparent age may therefore be better thought of as a something approximating the residence time, which for the major ions (Na, Cl, Mg, SO_4) that were the primary focus of these studies, are about 12–130 Ma.

The golden years of the late 19th century for speculative calculations bearing on the age of the Earth also saw estimates based on orbital physics. Around 1879, George Darwin, second son of Charles and most famous for the fission model of the origin of the Moon and creation of the Pacific Ocean basin, developed a complicated set of geophysical arguments involving dissipation of tidal friction and its effect on slowing Earth–Moon rotation, coming up with a minimum estimate of around 56 Ma. This line of investigation was shared by several others including Lord Kelvin himself, who constrained the problem to an age less than about 1 Ga.

Probably few approaches of the pre-radioactivity era received more attention as avenues for estimating geologic time than accumulation rates of sediments or sedimentary rocks. According to *Dunbar* [1949] the great historian Herodotus (484–425 BCE) attempted to understand durations through observing sediment deposition during flooding of the Nile. Extrapolating individual flood events to the sediment pile in the Nile delta he inferred that buildup of the sediment there must have taken thousands of years. He also discusses calculations of durations of time from a statue of Ramses II (about 3200 years old) buried beneath about 2.7 m of sediment, and the burial of a clearly much older burned brick about 12 m beneath the surface. He observed that this made sense with the observed deposition rate from the area of about 9 cm/century, suggesting a sensible uniformitarian approach could at least extend back several thousand years.

One of the most detailed and influential attempts to constrain the magnitude of geologic time was Charles Walcott's 1893 paper in the Journal of Geology. His opening lines characterize the debate at the time:

> "*OF ALL subjects of speculative geology few are more attractive or more uncertain in positive results than geologic time. The physicists have drawn the lines closer and closer until the geologist is told that he must bring his estimates of the age of the earth within a limit of from ten to thirty millions of years. The geologist masses his observations and replies that more time is required, and suggests to the physicist that there may be an error somewhere in his data or the method of his treatment.*"

Walcott divided sedimentary strata of the US Cordillera into clastic and chemical precipitated rocks (in this case limestones). But rather than use arguably more direct estimates of depositional rates extrapolated from short timescales of modern observations as Herodotus did, he employed relatively complex

Period.	Time Duration.
Cenozoic, including Pleistocene	2,900,000 years
Mesozoic	7,240,000 "
Paleozoic	17,500,000 "
Algonkian	17,500,000 "
Archean	10,000,000(?)"

Fig. 1.1. Estimated durations of time assigned to each geological era by Walcott based on stratigraphic accumulation (and erosion rate) estimates and observations from the US Cordillera. (Source: *Walcott* [1893].)

arguments about rates and areas of erosion providing the raw materials for deposition. Comparing these with thicknesses of stratigraphic units in each of the paleontologically defined eras, he came up with estimates shown in Fig. 1.1 (The Algonkian is essentially the same as the modern Proterozoic). Although the durations are obviously grossly low, it is interesting that the ratios of their apparent durations (except for the Archean and Algonkian, for which there was little sedimentary record in the region that Walcott could observe) are similar to those recognized now.

After Walcott's introduction, cited above, that contrasted geologic versus physics-based approaches, it is somewhat ironic that his estimate for the total duration of Earth history was not very different from that of Kelvin's. Many other estimates based on sediment accumulation were also published in the latest 19th and earliest 20th centuries, and although there were a few exceptions, by far most of them consistently estimated durations and total ages roughly 10 to 100 times too short. While some of this may owe to apparent legitimacy arising from similarities to physics-based methods, it is also undoubtedly an inevitable outcome of failure to properly account for unconformities, recycling, varying depositional (and erosional) rates, the fact that individual basins neither survive nor receive sediments for all of Earth history, and the increasing paucity of the preserved stratigraphic record for progressively older units. Although most of these limitations were recognized, their magnitude was obviously difficult to constrain, so when assumptions were made that yielded final results of the same order of magnitude as previous ones, those were probably considered the most reasonable.

In some ways, the relatively young field of geology of the late 19th to early 20th centuries was not held back by an inability to assign numerical ages to stratigraphic boundaries, deformation episodes, milestones of biotic evolution, or even the age of the planet. Armed with Nicolas Steno's principles of superposition and stratigraphic correlations, Cuvier's extinctions as marked by disappearances of fossil assemblages, and the ability to interpret orogenic episodes, there was a lot that could be done to interpret histories of subsidence, uplift, magmatism, deformation, and the regional extents and relationships of such processes. By 1870s, eras separated by biotic or lithologic differences were well defined (e.g., LeConte, 1879), including the Archaean (or Eozoic), Paleozoic, Mesozoic, Cenozoic, and the most recent era, the Psychozoic (which captures the defining characteristic of human degradation of our planet's habitability somewhat more eloquently than Anthropocene). The business of reconstructing the geologic history of the planet could, apparently, go on with only relative dating and some, at least relative, sense of the amount of time represented in each era.

But pre-geochronology geology floated in time and compressed Earth history the farther back in time one looked, underestimating the true extent of the planet's age by about 100 fold. This was at least partly due to the fact that the geologic record that was interpretable without geochronology was restricted to stratigraphic correlations of sedimentary rocks, particularly those bearing fossils. Correlations and interpretations of Precambrian rocks were difficult if not impossible without geochronology, and igneous and metamorphic units lacking constraints from related sedimentary rocks could be just about any age in any part of the world. Pre-20th century geologists recognized that there was a Precambrian history to the Earth, but the early "Geologic Timescale" basically ignored it. This is somewhat ironic not only because it excludes the vast majority of Earth history but also because the Precambrian–Cambrian boundary represents one of the most significant orogenic, biotic, and sedimentary events to affect the planet. Something huge happened at this time, but there was almost no way to date it or recognize how much time lay before it. In fact, because the Precambrian–Cambrian boundary represented a very widespread if not global event of very limited duration compared to the duration represented by the younger stratified rocks above it, it is an example of one of the completely undated but well-recognized geologic "revolutions" that proved useful for regional and global correlations and establishing the floating Geologic Timescale. According to *Williams* [1893],

> "*As the period of each dynasty in ancient history is marked by continuity in the successive steps of progress of the country, of the acts of the people and of the forms of government, and the change of dynasties is marked by a breaking of this continuity, by* revolutions *and readjustment of affairs, so in geological history the grand systems represent periods of continuity of deposition for the regions in which they were formed, separated from one another by grand revolutions interrupting the regularity of deposition, disturbing by folding, faulting and sometimes metamorphosing the older strata upon which the following strata rest unconformably and for the beginnings of a new system.*"

Geologic revolutions of the late 19th century included the close of the "Archean" revolution, now recognized as end of the Precambrian, as well as the Appalachian revolution (also recognized in Europe by other names), the Palisades revolution of the Jurassic–Triassic, the Rocky Mountain revolution (which was extended over what might now be a disturbingly long period of time, Cretaceous to Miocene, and also apparently distance, as lumped in causally were also the Pyrenees and the Himalaya), and the Miocene Cascadian revolution in flood basalts of the Pacific Northwest. Of course all of these periods were floating in temporal space. The clear and practically instinctive association

of numerical ages to geologic periods or eras that we enjoy now did not exist then, and these revolutions could have been millions to tens to hundreds of millions of years old.

By Dunbar's time in the early 20th century, after the discovery of radioactivity but before geochronology had a serious influence on mainstream geologic thinking, revolution concepts were still important bases of understanding, though they had been tweaked a bit. The Rocky Mountain disturbance had been separated into the Nevadan, peaking in the Late Jurassic, the Laramide, near the Cretaceous–Paleogene boundary, the Palisades had been relegated to a "disturbance," the Appalachian was seen to postdate two earlier disturbances, the Acadian and Taconian, and several revolutions were recognized within the Precambrian, the Penokean, Algoman, and Laurentian.

As useful as the concept of geologic revolutions were, most them were not nearly as global or even superregional as typically envisioned, and to a large degree reflected regional tectonic processes largely restricted to the stomping grounds of their investigators. Ironically, the arguably most globally preserved revolution, the Precambrian-Cambrian boundary, did not really rise to the status of a revolution because it represented such a fundamental shift in the rock record as to make it different from all the others. In any case, as late as the early 20th century there was general acceptance that very widespread "events" punctuated the stratigraphic record and therefore Earth history. Although few if any of these retain their nearly global significance, they do point out that even prior to the advent of geochronology there was a great deal known about the geologic record of the last ~542 Ma, even if it was entirely floating in time. Though reliable numerical ages were a long way off and the methods of estimating durations were primitive, some semi-quantitative constraints on the relative amounts of time represented by geologic periods were also available. J.D. Dana did this by assigning sedimentary thicknesses a standard unit of time, and proposing that an equivalent thickness of limestone (which was supposedly much slower to accumulate) represented 5 times the duration of other sedimentary rocks. Williams and LeConte extended this to the idea of the geochrone as a unit of time useful for correlations and fundamental counting tool. As an aside it was also Williams who in 1893 was the first to propose the term geochronology, with a somewhat puzzling emphasis to modern ears that the time concerned is not human-centric:

> "*In all these studies in which the geological time-scale is applied to the evolution of the earth and its inhabitants, the time concerned is not human chronology but is what may be called geochronology.*"

In some ways the geochrone is not a complete anachronism but is still used today. But instead of referencing time to a particular thickness of sedimentary rocks (e.g., the Eocene section in a specific place, as proposed by Williams), it is the orbital period of the Earth around the Sun, 1 year, or 365.256363004 days, or in SI units, 31558149.8 s.

Geochrones, geologic revolutions, and stratigraphic correlations allowed a great deal of Earth history to be reconstructed. The fact that the resulting structure was floating in time did not seem to be of paramount importance, and in fact even the significance of assigning numerical constraints to dates and rates of geologic events and processes any older than a few thousand years was often considered (as it still is by some practically-minded stratigraphers) as wading into a kind of speculative philosophy not unlike asking what existed prior to the big bang.

As late as the 1889 fifth edition of *Elements of Geology*, the renowned Joseph LeConte wrote:

> "*Previous to even the dimmest and most imperfect records of the history of the earth there is, as already said, an infinite abyss of the unrecorded. This, however, hardly belongs strictly to geology, but rather to cosmic philosophy. We approach it not by written records, but by means of more or less probable general scientific reasoning.*"

and

> "*Thus the history of the earth, recorded in stratified rocks, stretches out in apparently endless vista. And still beyond this, beyond the recorded history, is the infinite unknown abyss of the unrecorded. The domain of Geology is nothing less than (to us) inconceivable or infinite time.*"

Meanwhile, a few enterprising German and French scientists in the field that had underestimated the age of the Earth for so long were busy in labs doing experiments whose sometimes serendipitous results would move these questions from philosophy to hard science and begin a scientific and in some ways cultural revolution.

1.3 RADIOACTIVITY

In a universe with only slightly different physics, a conceivable combination of circumstances like the availability of still extant radioactive parent nuclides, the happenstances of trace element partitioning in common minerals, and the achievable precision of mass spectrometers might conspire to make radioisotopic geochronology impossible or at least much more difficult than it is. An almost uncomfortably small number of parent-daughter decay systems (Table 1.1) have decay constants and parent-daughter partitioning that make them geochronologically useful. And an almost absurdly large amount of what is known about the age of the Earth and terrestrial rocks in general comes from the U–Pb system alone. The parent isotopes of this system, ^{235}U and ^{238}U, have already lost 98.5% and 50%, respectively, of their abundance since the beginning of the solar system, and the technique is most often applied to a mineral, zircon, that constitutes only a fraction of a percent in certain rock types. If it weren't for nuclear transmutation and its manifestations in minerals with particular properties, except for the distant limits from astronomers and lifetimes of main-sequence stars, we may still be arguing

Table 1.1 Geochronologically useful radioactive decay systems

Parent/daughter (system)	Reaction or key daughters	Decay constant (a^{-1})	Half-life (a)	Daughter ratio typically measured
$^{147}Sm/^{143}Nd$	${}^{147}_{62}Sm \rightarrow {}^{143}_{60}Nd + {}^{4}_{2}He$	6.54×10^{-12}	1.06×10^{11}	$^{143}Nd/^{144}Nd$
$^{238}U/^{206}Pb$	${}^{238}_{92}U \rightarrow {}^{206}_{82}Pb + 8{}^{4}_{2}He$	1.55×10^{-10}	4.47×10^{9}	$^{206}Pb/^{204}Pb$, $^{207}Pb/^{206}Pb$
$^{235}U/^{207}Pb$	${}^{235}_{92}U \rightarrow {}^{207}_{82}Pb + 7{}^{4}_{2}He$	9.85×10^{-10}	7.07×10^{8}	$^{207}Pb/^{204}Pb$, $^{207}Pb/^{206}Pb$
$^{232}Th/^{208}Pb$	${}^{232}_{91}\mathrm{Th} \rightarrow {}^{208}_{82}Pb + 6{}^{4}_{2}He$	4.95×10^{-11}	1.4×10^{10}	$^{208}Pb/^{204}Pb$
(U–Th–Sm)/He	Sum of four above			$^{4}He/^{3}He$
$^{87}Rb/^{87}Sr$	${}^{87}_{37}Rb \rightarrow {}^{87}_{38}Sr + {}^{0}_{-1}\beta$	1.42×10^{-11}	4.88×10^{9}	$^{87}Sr/^{86}Sr$
$^{187}Re/^{187}Os$	${}^{187}_{75}Re \rightarrow {}^{187}_{76}Os + {}^{0}_{-1}\beta$	1.67×10^{-11}	4.16×10^{10}	$^{187}Os/^{188}Os$
$^{40}K/^{40}Ca$	${}^{40}_{19}K \rightarrow {}^{40}_{20}Ca + {}^{0}_{-1}\beta$	4.96×10^{-10}	1.25×10^{9}	$^{40}Ca/^{44}Ca$
$^{40}K/^{40}Ar$		0.581×10^{-10}	1.25×10^{9}	$^{40}Ar/^{36}Ar$
^{238}U/fission	Variable daughters + fission track	8.45×10^{-17}	8.20×10^{15}	Track density/^{238}U
$^{138}La/^{138}Ce$	${}^{138}_{57}La \rightarrow {}^{138}_{58}Ce + {}^{0}_{-1}\beta$	6.80×10^{-12}	1.02×10^{11}	$^{138}Ce/^{136}Ce$
$^{138}La/^{138}Ba$	${}^{138}_{57}La \rightarrow {}^{138}_{56}Ba + {}^{0}_{+1}\beta$	6.80×10^{-12}	1.02×10^{11}	
$^{176}Lu/^{176}Hf$	${}^{176}_{57}Lu \rightarrow {}^{176}_{56}Hf + {}^{0}_{-1}\beta + v$	1.87×10^{-11}	3.71×10^{10}	$^{176}Lu/^{177}Hf$
^{238}U series	Commonly used daughters: ^{234}U, ^{230}Th, ^{226}Ra, ^{210}Pb, ^{210}Po	$0.01–2.82 \times 10^{-6}$	1.00×10^{2} to 2.46×10^{5}	($^{234}U/^{238}U$), ($^{230}Th/^{238}U$), ($^{226}Ra/^{230}Th$), ($^{210}Pb/^{226}Ra$), ($^{210}Po/^{226}Ra$)
^{235}U series	Commonly used daughters: ^{231}Pa, ^{227}Ac	$0.03–2.12 \times 10^{-5}$	$22.8\text{-}3.28 \times 10^{4}$	($^{231}Pa/^{235}U$), ($^{227}Ac/^{231}Pa$)
^{232}Th series	Commonly used daughters: ^{228}Th, ^{228}Ra	0.12–0.36	1.92–5.75	($^{228}Th/^{232}Th$), ($^{228}Ra/^{232}Th$)

about the age of the Earth and solar system, or relegating such discussions to cosmic-philosophy as was common less than one hundred years ago. But fortunately, there are sufficient numbers of geochronologically useful decay systems, undecayed parents, and minerals available to us.

The first graying of the dawn of the nuclear era is usually associated with Wilhelm Conrad Roentgen's discovery of X-rays in Wurzburg, Germany in 1895. Although not due to natural radioactivity, his discovery of radiation that had the ability to penetrate most solids (c.f., the X-ray image of Roentgen's wife's hand complete with wedding ring) set the stage for an even more serendipitous and portentous discovery in the next year. In spring of 1896 Henri Becquerel performed a series of experiments in which he determined that uranium-bearing salts had the ability to darken photographic plates. His own iconic figure features a fuzzy image of two rectangular dark spots on a plate, corresponding to photographic impressions left by two plates coated in uranium-bearing salt; one of the rectangles shows a lighter region corresponding to a Maltese cross that Becquerel placed between the salt and photographic plates to demonstrate the lesser penetration through the iron (Fig. 1.2). Interestingly, very similar experiments had actually been done and observations made about 40 years before this, by a French photographic inventor with the impressively lengthy name Claude Félix Abel Niépce de Saint-Victor, who noted that uranium produces "a radiation that is invisible to our eyes." In fact, Henri Becquerel's father Edmond had written about these observations in his book about light published in 1868.

Less serendipitous and more deliberate systematic explorations into natural radioactivity and a series of foundational discoveries

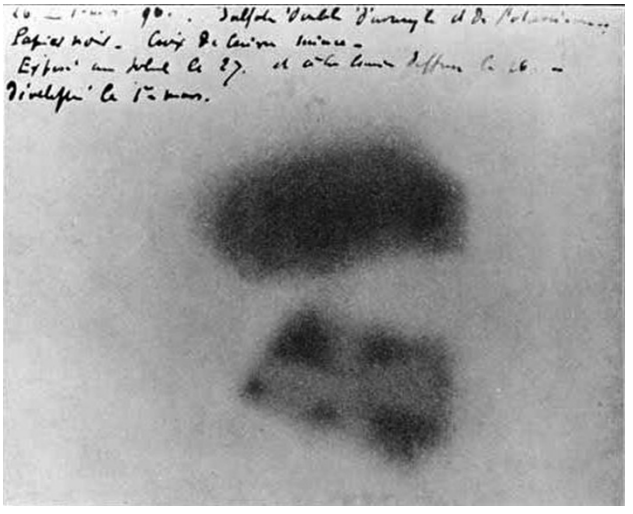

Fig. 1.2. Henri Becquerel's 1896 image of a photographic plate exposed by natural radiation from uranium-bearing salts. The lower of the two shows the shadow of an iron Maltese cross placed between the sample and the plate. (Source: https://en.wikipedia.org/wiki/Henri_Becquerel#/media/File:Becquerel_plate.jpg)

by Marie, and later Pierre, Curie soon followed Becquerel's work. Marie Curie measured electrical charge on the air surrounding uranium, and observed that its extent depended only on the amount of uranium present, leading to a hypothesis that uranium's radiation came from the atom, not molecules. She also observed that other U-bearing minerals were far more radioactive than uranium, leading to the insight that other elements must also be radioactive. Although she is often credited with discovering that Th is also radioactive, this was actually published in Berlin two months before by Gerhard Carl Schmidt. However,

her more important insight, that uranium minerals contain small amounts of much more radioactive elements, soon led her and Pierre to large-scale chemical separations of constituents of uraninite (pitchblende), and the discovery of polonium and radium and recognition of their highly radioactive nature. In 1903 Marie and Pierre Curie (Fig. 1.3) and Henri Becquerel won the Nobel Prize in Physics; Marie also won a second prize in 1911 for her work on radium; their daughter Irène Joliot-Curie also won the Nobel in 1935 for discovery of artificial (neutron-bombardment induced) radioactivity.

The Curie's work on radioactivity accelerated progress on natural radioactivity at the turn of the century. In 1899 the Kiwi physicist Ernest Rutherford (Fig. 1.4) distinguished two types of radiation with different penetrating powers that he termed alpha and beta. He also discovered that thorium produced a gas, or "emanation" as he called it, that was itself radioactive, and that the activity of this gas followed a law whose differential form is $dN/dt = -\lambda N$, establishing the concept of the radioactive decay constant and half-life, which he determined for Th-emanation (now known to be ^{220}Ra) as 60 s (not far from today's accepted value of 55.6 s). In the process he also noticed that Th-emanation itself eventually produced another radioactive substance, which we now recognize as ^{212}Pb.

Working together between 1900 and 1903, *Rutherford and Soddy* [1903a,b] further characterized other intermediate daughter products of the U- and Th-series (as did several other workers of the time), suggested that He could be a decay product of radium, and they developed the "atomic theory of disintegration" that proposed radiation as a byproduct of "spontaneous transformation" of atoms of one element into those of another. They also delineated part of the first U- and Th-series decay series chain, and mathematically described its behavior (Fig. 1.5);

Fig. 1.3. The 1903 Nobel Prize winners Marie and Pierre Curie as depicted on the French 500-Franc note. (*See insert for color representation of the figure.*)

Fig. 1.4. The 1908 Nobel Prize winner Ernest Rutherford as depicted on the New Zealand 100-dollar note. (Source: https://commons.wikimedia.org/wiki/File:100Neuseeland-Dollar_vorderseite_21585256953_02d6c65788_o.jpg. Used under CC BY SA 3.0.). (*See insert for color representation of the figure.*)

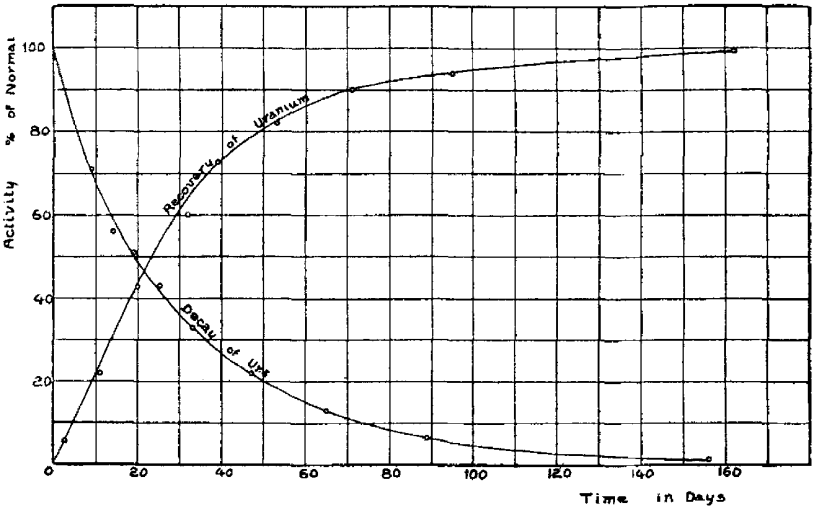

Fig. 1.5. Original figure from *Rutherford and Soddy* [1903b]. The curve showing an increase with time is the beta-activity of uranium from which a then unknown substance called uranium-X (now recognized as ^{234}Th) had been chemically removed, and the decreasing curve is the activity of the separated uranium-X. Through this experiment Rutherford and Soddy estimated the half-life of U-X (^{234}Th) as 22 days (now known to be 24.10 days) and recognized the beginning of the ^{238}U decay chain. (Source: *Rutherford* [1903]. Reproduced with permission of Taylor & Francis.)

this was followed up in a more complete way by *Harry Bateman* [1910], who laid out the differential equations and solutions for chained decay systems.

The year 1905 is sometimes referred to as the *annus mirabilis* for publication of Albert Einstein's four foundational physics papers, including the one with the famous equation relating nuclear energy, mass, and the speed of light. But it also was not a bad year for the study of radioactivity and geochronology. New Haven chemist Bertram Boltwood noted that Pb was likely a decay product of U, and in a series of lectures at the World's Fair in St. Louis and also at Yale, Rutherford presented a calculation of the first radioisotopic age. He described the calculation in a 1905 publication. Because the rate of He production directly from U was not known, but the Ra to He production was, Rutherford combined an assumption of U–Ra secular equilibrium with He and U concentrations, measured previously by William Ramsay and Morris Travers, on a sample of fergusonite, a Nb–Ta oxide, to obtain an apparent age of about 40 Ma [*Rutherford*, 1905]. In his book *Radioactive Transformations* [1906] he uses a different Ra to He production rate to obtain an age on the same sample of about 500 Ma, which he noted was likely a minimum as some of the He may have escaped. In the same work he also calculated 500 Ma for a uranium-bearing mineral from Glastonbury, Connecticut analyzed by W.F. Hillebrand. For some reason these calculations were undertaken assuming a simple linear relationship between the U (Ra) and He concentrations and Ra decay rate, even though Rutherford was aware of, and in fact derived with Soddy, the mathematical descriptions of radioactive decay and growth several years earlier.

Interestingly, in his 1906 book Rutherford also described W.F. Hillebrand's observations that U/He (though Hillebrand thought, as others prior to about 1902, that the inert gas in U-bearing samples was N_2, not He) ratios appeared to be fairly constant for "primary" minerals in certain locations but different from U/He ratios of similar minerals in other places. Given that Rutherford recognized the likelihood that some fraction of radiogenic He is lost from samples over time, the attention he pays to this observation suggests that he recognized the potential of the U–He system to represent something about regional geologic histories.

Although the accuracy, precision, and exact geologic significance of these first radioisotopic ages are not clear, their symbolic scientific importance was huge. Simple as they were, they were literally the first time humans resolved the timing of *something* in deep time using fundamental physical foundations relying only on uniformitarianism of decay constants. The ages came with a kind of cosmic insight that had been missing from centuries of "scholarly reasoning," wishful thinking, semi-quantitative heurism, and floating timescales. The fact that two almost arbitrary mineral samples from different places yielded ages about an order of magnitude older than prevailing estimates for the age of the entire Earth must have suggested to some that either the physics was missing something and the method was completely useless, or that physics had just provided something like a Promethean lens with which to understand the Earth and universe in an entirely new and powerful way.

Also in 1905, and in rapid succession over the next few years, Robert John Strutt (later the 4th Baron Rayleigh) published a large number of analyses and calculated ages of minerals and related materials based on the relative concentrations of He, U and Th, the latter which Strutt recognized as also producing radiogenic He. Strutt noticed that (U–Th)/He ages of specimens thought to be from the same geologic stratum in different places yielded different apparent ages, and that many samples lost He at room temperatures at rates approaching, and in some cases higher than, their production rates. This He "leakage" rendered the method largely unusable for the tasks of the day, which were to establish the age of the Earth and to place reliable numerical estimates on key parts of the geologic timescale.

Around the same time, Bertram Boltwood, a prolific scientific penpal of Ernest Rutherford [*Badash*, 1969], carried out experiments showing that Pb was likely the end-product of decay of U. Using the reasoning that the number of decays of U to Ra was the same as the number of decays of Ra to Pb (i.e., secular equilibrium), Boltwood calculated an apparent decay rate of U (around 1×10^{-10} a^{-1}), and combined this with measured U/Pb ratios in a series of minerals from a variety of areas, coming up with ages ranging from 410 Ma (for a sample from Glastonbury, Connecticut) to 2.2 Ga. If Rutherford's initial ages were in essence thermochronologic ages, Boltwood's were the first real geochronologic age estimates, insofar as they came closer to estimating formation rather than potential cooling ages.

Recognizing that Pb provided a more promising daughter product than He for measuring formation ages, one of Strutt's most famous students, Arthur Holmes, began a long series of studies carefully characterizing U/Pb ratios and apparent ages of a wide variety of samples strategically chosen from various parts of the geologic timescale. Initial results, published in 1911, carried a lot of promise for the new U/Pb dating method, showing regionally and stratigraphically consistent ages (Fig. 1.6).

Somewhat surprisingly, given geologists' decades of kvetching that physicists had the age of the Earth far too young, radioisotopic geochronology did not catch on quickly in geology. Once ages of many minerals were starting to look one to two orders of magnitude older than mainstream physicists' estimates, it was the geologists who generally became skeptical of the whole approach. Many proposed variable decay rates as a most probable culprit. Two US Geological Survey geologists led the skepticism prominently. *George Becker* [1908] measured U/Pb ratios of altered uranium minerals in Texas, finding apparent ages in some cases older than 10 Ga, prompting him to reiterate earlier arguments based on oceanic sodium accumulation and terrestrial "refrigeration" (à la Kelvin) that made these new estimates essentially untenable [*Becker*, 1910]. Even as late as 1924, the famous geochemist Frank Wigglesworth Clarke (with Henry Washington) cast copious doubt on radioisotope methods because they appeared to be so discordant with earlier methods that seemed

The Association of Lead with Uranium in Rock-Minerals.

Geological period.	Pb/U.	Millions of years.
Carboniferous	0·041	340
Devonian	0·045	370
Pre-carboniferous	0·050	410
Silurian or Ordovician	0·053	430
Pre-Cambrian—		
a. Sweden	0·125	1025
	0·155	1270
b. United States	0·160	1310
	0·175	1435
c. Ceylon	0·20	1640

Fig. 1.6. Table of early U/Pb ages. (Source: *Holmes* [1911].)

to converge in the much more "reasonable" tens to (maximum!) hundred Ma age range.

Although dating based on radioactive decay had a long way to go before mainstream acceptance, it was pursued in the early 20th century by a number of pioneering geologists with clever ways of estimating ages from U/Pb chemical dating. In 1917, Joseph Barrell made the first real attempts at delineating the boundaries between the main geologic eras, in his poetic and prescient publication "Rhythms and the measurement of geologic time." Aside from discussing what we now call Milankovitch cycles and climatic influences on sedimentation, he came pretty darn close (especially considering the tools and data available) to the currently recognized era boundaries: Cenozoic–Mesozoic at 55–65 Ma, Mesozoic–Phanerozoic at 135–180 Ma, and Phanerozoic–Precambrian at 360–540 Ma.

Attempts to use radioactivity to hone in on the age of the Earth itself started to approach at least the right order of magnitude, for the right reasons, with Henry Russell, an astronomer, who used relative concentrations of radioactive and radiogenic elements in the Earth's crust. His best estimates came up with a maximum age of about 8 Ga from U, Th, and Pb concentrations, and a minimum of about 1.1 Ga, from the oldest U/Pb age on minerals that he considered reliable.

As the era of radioactive "chemical" dating came to a close near the end of the 1920s, the geochronologic giant Arthur Holmes redid Russell's calculations, using U, Th, and Pb concentrations in the crust to estimate a most likely age of 1–3 Ga for the Earth [*Holmes and Lawson*, 1927]. He also amassed a good deal of previous data to delineate ages for various parts of the geologic timescale, and compared estimates from various methods.

With increasing convergence of an increasing number of calculations pointing to ages in the 1–3 Ga age range, and with the official authoritative blessing of an National Research Council committee report appointed by the National Academy of Sciences in 1931, the question of the age of the Earth appeared to have been solved (though not to all geologists, by any means) to at least an order of magnitude, and probably a factor of a few.

In the middle part of the 20th century, further progress in geochronology received a huge boost from the proliferation of mass spectrometry, begetting truly radioisotopic geochronologic methods. The recognition that some elements comprised atoms with more than one mass is generally attributed to Frederick Soddy. The name isotope referred to the fact that two different types of an element occupy the same place in the periodic table, and is said to have been suggested to him by novelist and medical doctor Margaret Todd during a dinner party in Glasgow. An example of the observations behind this insight go at least as far back as Boltwood's 1906 notes that a decay product of uranium, then called ionium and now known to be ^{230}Th, was chemically identical to thorium (i.e., ^{232}Th).

Ernest Rutherford's former advisor, J.J. Thomson, is generally given credit as the first one to separate isotopes of an element by mass spectrometry, identifying ^{20}Ne and ^{22}Ne in 1913. Another student of Thomson's, Francis Aston, built a mass spectrometer for the purpose of separating nuclides based on mass-to-charge ratios, and he identified multiple isotopes of Cl, Br, and Kr, earning a Nobel Prize in 1921. By 1929 Aston had measured the isotopic composition of radiogenic Pb in a Norwegian sample of broggerite (Th-bearing uraninite) and showed it to have much higher proportions of ^{206}Pb and ^{207}Pb than common Pb. Besides attributing the ^{206}Pb to U decay, he noted that the ^{207}Pb must have come from a precursor with an atomic mass of about 231, naming this element protactinium (actinium had actually been discovered much earlier, by DeBieren in 1899). Immediately following Aston's discovery, Fenner and Piggot were the first to use radioisotopic compositions of an element to calculate ages, combining the ^{206}Pb–^{207}Pb and ^{208}Pb abundances with the U and Th contents of the same sample analyzed by Aston, to obtain apparently discordant ages of 908 and 1310 Ma for the U–Pb and Th–Pb systems, respectively.

Also in 1929, Rutherford proposed that the parent of Aston's protactinium (actino-uranium) was likely to be a uranium isotope with a mass number of 235. After estimating the decay constant of the new element, he calculated the amount of time that would

be required to reduce an assumed $^{235}U/^{238}U$ value of unity (as a heuristic assumption for an initial value in the solar nebula) to the present value, which he estimated as about 0.28%. His answer, which he presumed provided a constraint on the time since the Earth separated from the Sun, was 3.4 Ga (although using the now more accurately known constants this becomes 5.9 Ga). Rutherford noted that this was approximately twice as old as previous U/Pb age determinations on any terrestrial sample. This was the first constraint on the age of the Earth from isotopic compositions. (As an aside, in the same paper, Rutherford then used a contemporary accepted age estimate for the Sun (of seven trillion years), to infer that the Sun must have been able to produce uranium at least as recently as about 4 Ga, and probably still does today…).

Dramatic improvements in mass spectrometry occurred through the 1930s and 1940s, driven largely by concerns quite different from determining the age of the Earth and its rocks, primarily nuclear physics and the Manhattan Project. Applications to Pb isotopic compositions led quickly to generally converging estimates of the age of the Earth in the 2–4 Ga range. Alfred Nier, at the University of Minnesota, measured Pb isotopic compositions of both Pb ores (low U/Pb) and uraniferous (high U/Pb) samples from a variety of locations. Besides calculating ages of many samples that supported the existence of minerals with ages older than several billion years, he proposed that Pb isotopic variations could arise from separation of materials from primordial Pb into reservoirs with a range of U/Pb ratios over time. In 1942, E.K. Gerling, who also pioneered interpretation of diffusion kinetics of noble gas thermochronometry well ahead of his time, used this approach and Nier's measurements to develop some of the first Pb-dating approaches that became widespread in subsequent decades. Using a combination of minerals dominated by radiogenic and ore Pb, he used complex but prescient arguments to establish durations of time required to generate Pb isotopic differences, including a minimum estimate of 3.94 Ga for the Earth.

Somewhat similar approaches to estimating durations required for generating Pb isotope differences were also taken, independently, by Holmes and Houtermann through the 1940s and 1950s, obtaining constraints generally pointing to 3–4 Ga ages. As technically robust as many of the analyses were, and as insightful and useful as they were for understanding common Pb behavior in the crust, they required assumptions about source homogeneity, isolation of reservoirs, and durations of "events" that separated these reservoirs that limit their ability to accurately constrain the age of the Earth beyond the prevailing convergence of approximately 3–4 Ga.

Clair Patterson's famous 1956 paper "*Age of meteorites and the Earth*," was similar but introduced a significant variation on the Pb isotope riff, introducing the age of meteorites into the question. In an elegant two-figure paper, Patterson combined primitive Pb isotopic compositions of meteoritic (Canyon Diablo) troilite with that of several other meteorites. He showed that these meteorites form a single isochron consistent with

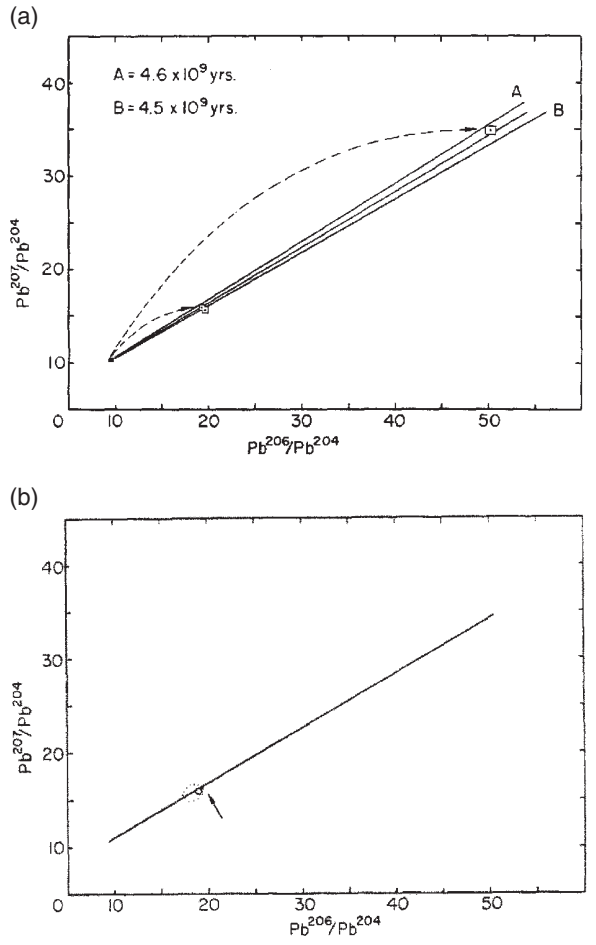

Fig. 1.7. (a) Pb-isotopic compositions of five meteorites. The least radiogenic point (near 10,10) represents troillite analyses from two different metallic meteorites; the other three points are from stony meteorites. The central line is the regression through the meteorite points; A and B represent isochrons with ages shown in legend. Curved dashed lines represent the evolution of Pb-isotopic compositions with time inferred for closed-system sources derived from the same reservoir as the troillite point. (b) The reference meteorite isochron compared with the Pb isotopic composition of oceanic sediment (unfilled circle) and a selection of recently formed galena ores (dashed field). (Source: Figures 1 and 2 from *Patterson* [1956]. Reproduced with permission of Elsevier.)

fractionation of U and Pb about 4.550 ± 0.070 Ga and closed system behavior since then (Fig. 1.7). Rather than comparing this isochron with numerous terrestrial samples, he then argued that a convenient proxy for the bulk common Pb composition of Earth could be estimated by oceanic sediment, which was rather close to many galena ores. Patterson may have been motivated to use oceanic sediment, distant from anthropogenic sources, partly because of his other work demonstrating the widespread Pb contamination of natural environments from burning of leaded gasoline. Although we now understand that even natural Pb-isotopic compositions of oceanic sediment vary more widely than the small range represented by Patterson, however fortuitous his sample choice was, the basic idea was not flawed. As long as one

accepted the cogenetic nature of the Earth and the meteorites he chose for this study, and the approximation of his oceanic sediment for the Pb isotopic composition of the bulk Earth, the question of the age of the planet was at least close to settled.

Since Patterson's time, older terrestrial rocks and minerals have been discovered and dated precisely and accurately and have provided important geological understanding. Examples include early Archean units in Greenland and the Acasta gneisses of northern Canada [e.g., *Moorbath et al.*, 1975; *Bowring et al.*, 1989], and the well-known Jack Hills detrital zircons of western Australia, some of which yield concordant ages as old as 4.4 Ga [*Compston and Pidgeon*, 1986; *Wilde et al.*, 2001]. As far as determining the age of the Earth, the problem is no longer inadequate chronometers, but instead recognizing that the formation of the Earth was not an instantaneous event, not even on the scale of chronological resolution provided by radioisotopic geochronometers. The circa 4.567 Ga crystallization ages of some components of meteorites can now be determined with precisions of tens of thousands of years, but Earth growth likely took tens of millions of years. The processes involved in growing the Earth were sufficiently energetic that they continually reset the radioactive clocks in ways that are not yet well understood. As a result, most attempts to determine a singular age for the Earth, such as Patterson's, provide, at best, something approximating an average age for the interval of Earth growth. While "four and a half billion years" likely will remain a valid answer for the general age of the Earth, we can now ask this question in more detail. For example, when did Earth acquire its bulk composition, when did it form its core and atmosphere, and when did it form its first crust? Much like how the principle of superposition allowed resolution of the processes involved in the growth of sedimentary deposits, the precision obtainable with modern geochronometers is allowing the decoding of the processes involved in the growth of the Earth as a planet.

1.4 THE OBJECTIVES AND SIGNIFICANCE OF GEOCHRONOLOGY

Much of the preceding review focuses on the ability of geochronology to address ostensibly simple problems like the age of the Earth and of stratigraphic boundaries, and the history of those challenges as if they were linear pursuits with clear endings defined by sufficiently small error bars on a single number. It is true that the age of the Earth and of the punctuations in its biotic evolution are of great importance. As Martin Rudwick, and Steven J. Gould before him, suggested, the discovery of deep time and the historical evolution of the Earth and its inhabitants requires a cognitive expansion in human perspective beyond the generations, revolutions, and rises and falls of civilization, and therefore another displacement of humanity as the center of the universe, in this case with respect to time.

But as important as these questions are, geochronology is not just about determining the age of the Earth, marking precise mileposts on the geologic timescale, or even simply dating more geologic "things." If it were it would be an anachronism, minimizing its significance by its own progress—an exercise of increasingly specific, local, or minute geologic features. Simple questions posed as problems for hyperprecise dating raise the question of just how abrupt or well-defined events or processes are in the first place and so how precisely they could ever be known. Fortunately, questions that start out as easily posed usually do not end up that way. The Earth did not instantaneously appear, but was accreted over time, possibly with significant episodic mass loss, not to mention differentiation episodes; all these continue today, complicating questions of when. Similarly, stratigraphic boundaries are almost certainly diachronous to some degree, and the question of how diachronous they are may be at least as interesting as their regionally averaged age. For example, one could imagine that the K–P boundary may be diachronous over hours, whereas others defined by evidence for biostratigraphic changes that are less catastrophic may be over millions of years. The most interesting questions may have fundamental temporal aspects, but they are not solved by determining a single number with units of time.

Besides questions of instantaneousness and diachroneity, geochronology as a science in its own right comes from questions about not just dates, but also durations, rates, frequencies, and fluxes of geologic and planetary processes. Time is a fundamental characteristic of any natural process, and in many cases a timescale of some kind may be the most important part of understanding the process. For example, in struggling with the question of geochrones and stratigraphic durations, geologists of the pre-radioactivity era struggled with much more fundamental and physically enlightening questions: how long does erosion take; how long does sedimentation take? Why does it vary and what does that tell us? How long does it take to build a volcano, crystallize a pluton, or for groundwater to move through an aquifer? How steady or episodic are these processes and so over what timescales and length scales do these rates actually have a useful answer? Are these even reasonable questions with clear answers of the kind we are asking, or are these processes more complex than recognized by our simple questions? For example is groundwater transport far more complicated than can be expressed by a simple velocity, or will the attempt to answer the question lead to insights about episodicity of fluxes, mixing with ancient or multi-sourced fluids, dewatering and sorption with subsurface minerals, etc.? Although it is sometimes used this way, the objective of geochronology is not simply to estimate or deduce simple ages with which to label predefined geologic features as if the only thing left to understand is their birthdays. Geochronologic studies may start with simple questions, but most the power comes from harnessing the versatility of radioisotopic decay in analytically and interpretationally innovative ways. This often means resisting the temptation to declare that a geochronologic investigation "did not work." Unexpected geochronologic results are often interpreted as method failure, but the history of geochronology itself shows that these are often the most important results,

leading to critical insights into the behavior of the radioisotopic systems or the geologic processes themselves.

One simple interpretation of a date is closure of the sample (a crystal, rock, fluid, etc.) to gain or loss of parent and daughter nuclides (or "daughter" damage effects). In many cases this may be reasonably argued to correspond to closure, especially for systems involving relatively immobile parent and daughter elements and single crystals or parts of crystals. Some consider this "geochronology" in the strict traditional sense—dating the age of formation of a phase. But geochronology could also refer to the collective activities of constraining other types of ages, rates, durations, and thermal histories, and processes with a key temporal aspect.

In other cases, age interpretations benefit from the consideration of open system behavior of either the parent or the daughter subsequent to formation of the sample. In most cases it is the daughter that is more easily lost, and this leads to great utility in thermochronology, U-series, and cosmogenic methods, as the chapters in this book demonstrate. Preferential loss of a daughter product is not a coincidence: typically the most useful systems are those in which the parent/daughter ratio is high, and if this is true the parent "fits" well into the crystallographic structure relative to the daughter, most likely because of its ionic radius and charge, and is therefore partitioned into it. In contrast the daughter is less welcome in the structure and more likely to be lost if opportunity or disturbance (typically thermal) arises. Therefore when we talk about closure we mostly mean cessation of loss of daughter products. But there are exceptions to this: Lu/Hf in garnet for example: although Lu partitions into garnet more than Hf, Lu has a higher diffusivity so may migrate out during high-T events.

Open-system behavior of radioisotopic systems is often associated with migration of daughter products by thermally activated diffusion (or annealing). Thermochronologic applications resulting from this have a wide range of uses in both low and high temperature settings. In some cases, geochronologic ages may be associated with neither formation nor temperature change, but other kinds of processes. Exposure or burial ages, for example, are commonly the target of cosmogenic nuclide and luminescence or ESR studies. Compositional changes, such as diagenetic uptake of parent nuclides accompanying fossilization, hydrothermal activity, or the timing of comminution are targeted by some types of U-series or ESR dating. In many cases, geochronologic approaches do not yield a simple date, but instead some other kind of temporal constraint. In many cosmogenic or low-temperature thermochronologic studies, for example, ages themselves carry little meaning other than through their relationships among samples, which can yield spatial or temporal patterns of erosion. Many U-series studies provide not dates, but minimum or maximum durations of time since material transfer, phase changes, transport, or other processes that fractionate intermediate daughter products. Some groundwater studies of He and H isotopes aim for constraints not on dates but rates of movement through underground reservoirs. Sedimentation rates have traditionally been the target of ^{230}Th excesses in deep-sea sediment.

Highly directed applications of geochronology to specific objectives have a long and successful history: e.g., determining the age of the Earth, ultraprecise stratigraphic dates, and astrochronologic calibrations. Deliberate and strategic method developments also have a distinguished track record: e.g., the engineering of ^{40}Ar/^{39}Ar dating, ^{4}He/^{3}He diffusion experiments, intercalibration of decay constants, and precise measurements of cosmogenic production rates. But some of the most important results of geochronology have been exploratory or even serendipitous, even if our professional propensity to recast our findings as resulting from carefully designed strategic plans make this hard to recognize. Few other approaches in geoscience have the ability to yield surprising results with minimal effort. Relatively straightforward techniques for measuring ages can be easily and widely applied in exploratory ways, rather than highly considered or routine conventional ways. In context, exploratory geochronology has the potential to relatively easily reveal insights that we did not know we did not know, especially when datasets are conscientiously combined, in the manner of abductive discovery advocated by *Hazen* [2014].

Discovery in geochronology also comes from exploring physical and chemical behavior of the chronometric systems. Our actual mechanistic understanding of how parent and daughter elements (or features) behave in minerals lags far behind our geologic applications. The lag is not in the basic physics of decay and decay constants, which are well known. Rather, many aspects of our understanding of the isotopic systems that we use are highly heuristic models based on relatively simple observations of complex systems. While we make many assumptions about daughter (and parent) nuclide partitioning and behavior in (usually ideal, perfect lattices of) crystals, in reality our mechanistic understanding of nuclide behavior at the atomic scale and the effects of defects are quite primitive. New discoveries of radioactive and radiogenic nuclide behavior at the atomic scale are revealing how complex these systems can be, but also what incredible archives of planetary history these complications can reveal [e.g. *Kusiak et al.,* 2015; *Valley et al.*, 2015]. Surprising but powerful insights also come from the behavior of parents and daughters in cases where interphase partitioning, intragranular media, or fluids impart unexpected behavior [e.g., *Camacho et al.*, 2005]. Innovative geochronology of the terrestrial planets, an endeavor that is evolving from analysis of accidentally launched samples [e.g. *Shuster and Weiss*, 2005; *Zhou et al.*, 2013] to more deliberate sample return and dating *in situ* [*Farley et al.*, 2014], also holds great promise for experimenting, exploring, and discovering.

This book contains chapters on many (but not all) of the tools of the trade of geochronology, a field that has become incredibly diverse and powerful since Williams proposed the term in 1893. The chapters aim to provide a blend of history, theory, nuts and bolts, and applications, all in a modern outlook that raises questions and nudges towards innovation, for the various techniques.

What ties these chapters and techniques together is the underlying question of dates and rates. As geochronology has expanded and the applications and approaches have become so varied and versatile that many modern objectives are much more nuanced than simple formation ages, the common themes of radioisotopic decay and growth (along with nucleogenic and cosmogenic production), and the desire for more precise, accurate, and innovative approaches to understanding dates and rates of natural processes have created a kind of disciplinary cohesion that underscores the fundamental importance of time in Earth and planetary science. Although the approaches and applications in these chapters may be diverse and at least superficially distinct, even besides the isotopic bases, they have in common that they are keys to discovering, quantitatively, when and how fast. To paraphrase Lord Kelvin again, when you can measure that, and express it in numbers, you know something about it. Without the temporal context of time, your knowledge is of a meagre and unsatisfactory kind.

1.5 REFERENCES

Badash, L. (1969) Rutherford and Boltwood: Letters on Radioactivity. Yale University Press, 378 pp.

Barrell, J. (1917) Rhythms and the measurements of geologic time. *Geological Society of America Bulletin* **28** (1), 745–904.

Bateman, H. (1910) The solution of a system of differential equations occurring in the theory of radioactive transformations. *Proceedings of the Cambridge Philosophical Society* **15** (part V), 423–427.

Becker, G. F. (1908) Relations of radioactivity to cosmogony and geology. *Geological Society of America Bulletin* **19** (1), 113–146.

Becker, G. F. (1910) *The Age of the Earth*, Vol. **56**. Smithsonian institution.

Bouvier, A. and Wadhwa. M. (2010) The age of the Solar System redefined by the oldest Pb–Pb age of a meteoritic inclusion. *Nature Geoscience* **3**(9), 637–641.

Bowring, S. A., Williams, I. S., and Compston, W. (1989) 3.96 Ga gneisses from the Slave Province, Northwest Territories, Canada. *Geology* **17**(11), 971–975.

Brennecka, G. A., Weyer, S., Wadhwa, M., Janney, P. E., Zipfel, J., and Anbar, A. D. (2010) $^{238}U/^{235}U$ variations in meteorites: extant ^{247}Cm and implications for Pb–Pb dating. *Science* **327** (5964), 449–451.

Buffon, G.-L. L. (1778) *Les Époques de la nature: 1778*. Paleo.

Burchfield, J. D. (1975) *Lord Kelvin and the Age of the Earth*. Science History, New York.

Camacho, A., Lee, J. K. W., Bastiaan J. Hensen, B. J., and Braun, J. (2005) Short-lived orogenic cycles and the eclogitization of cold crust by spasmodic hot fluids. *Nature* **435**(7046), 1191–1196.

Chamberlin, T. C. (1899) On Lord Kelvin's address on the age of the Earth as an abode fitted for life. *Annual Report*, 223–246. Smithsoniam Institution, Washington, DC.

Clarke, F. W. and Washington, H. S. (1924) *The Composition of the Earth's Crust*, Vol. **127**. US Government Printing Office, Washington, DC.

Compston, W. T. and Pidgeon, R. T. (1986) Jack Hills, evidence of more very old detrital zircons in Western Australia. *Nature* **321**(6072), 766–769.

Dalrymple, G. B. (1994) *The Age of the Earth*. Stanford University Press, 474 pp.

Dunbar, C. O. (1949) *Historical Geology*. New York, 567 pp.

Farley, K. A., Malespin, C., Mahaffy, P., *et al.* (2014) *In situ* radiometric and exposure age dating of the Martian surface. *Science* **343**(6169), 1247166.

Fleischer, R. L. and Price, P. B. (1964) Techniques for geological dating of minerals by chemical etching of fission fragment tracks. *Geochimica et Cosmochimica Acta* **28**(10), 1705–1714.

Gerling, E. K. (1942) Age of the earth according to radioactivity data. In *Doklady (Proc Russian Acad Sci)*, **34**, pp. 259–261.

Guenthner, W. R., Reiners, P. W., Ketcham, R. A., Nasdala, L., and Giester, G. (2013) Helium diffusion in natural zircon: radiation damage, anisotropy, and the interpretation of zircon (U–Th)/He thermochronology. *American Journal of Science* **313**(3), 145–198.

Halliday, A. N., Lee, D-C., Christensen, J. N., *et al.* (1998) Applications of multiple collector-ICPMS to cosmochemistry, geochemistry, and paleoceanography. *Geochimica et Cosmochimica Acta* **62**, 6 919–940.

Hazen, R. M. (2014) Data-driven abductive discovery in mineralogy. *American Mineralogist* **99**(11–12), 2165–2170.

Holmes, A. (1911) The association of lead with uranium in rock-minerals, and its application to the measurement of geological time. *Proceedings of the Royal Society of London, Series A* **85**, 248–256.

Holmes, A. and Lawson, R. W. (1927) Factors involved in the calculation of radioactive minerals. *American Journal of Science* **76**, 327–344.

Kelvin, Lord. (1863) Dynamical problem regarding elastic spheroid shell; on the rigidity of the Earth. *Philosophical Transactions of the Royal Society of London, Treatise on Natural Philosophy* **2**, 837.

Kosler, J. (2008) Laser ablation sampling strategies for concentration and isotope ratio analyses by ICP-MS. *Laser Ablation ICP-MS in the Earth Sciences: Current Practices and Outstanding Issues* **40**, 79–92.

Kusiak, M. A., Dunkley, D. J., Wirth, R., Whitehouse, M. J., Wilde, S. A., and Marquardt, K. (2015) Metallic lead nanospheres discovered in ancient zircons. *Proceedings of the National Academy of Sciences* **112**(16), 4958–4963.

Lee, D-C. and Halliday, A. N. (1995) Hafnium–tungsten chronometry and the timing of terrestrial core formation. *Geochimica et Cosmochimica Acta* **62**, 919–940.

LeConte, J. (1879) Elements of Geology: a Text-book for Colleges and for the General Reader. D. Appleton and Company, New York.

Merrihue, C. and Turner, G. (1966) Potassium-argon dating by activation with fast neutrons. *Journal of Geophysical Research* **71**(11), 2852–2857.

Moorbath, S., O'nions, R. K., and Pankhurst, R. J. (1975) The evolution of early Precambrian crustal rocks at Isua, West Greenland—geochemical and isotopic evidence. *Earth and Planetary Science Letters* **27**(2), 229–239.

Patterson, C. (1956) Age of meteorites and the Earth. *Geochimica et Cosmochimica Acta* **10**(4), 230–237.

Rudwick, M. J. S. (2014) *Earth's Deep History: How it was Discovered and Why it Matters*. University of Chicago Press.

Rutherford, E. (1905) Present problems in radioactivity. *Popular Science Monthly* **67**.

Rutherford, E. (1906) *Radioactive Transformations*. Yale University Press.

Rutherford, E. (1929) Origin of actinium and age of the Earth. *Nature* **123**, 313–314.

Rutherford, E. and Soddy, F. (1903a) Radioactive change. *Philosophical Magazine* **5**, 576–591.

Rutherford, E. and Soddy, F. (1903b) XLIII. The radioactivity of uranium. *Philosophical Magazine* **6**, 441–445.

Shuster, D. L. and Weiss, B. P. (2005) Martian surface paleotemperatures from thermochronology of meteorites. *Science* **309**(5734), 594–600.

Shuster, D. L., Flowers, R. M., and Farley, K. A. (2006) The influence of natural radiation damage on helium diffusion kinetics in apatite. *Earth and Planetary Science Letters* **249**(3) 148–161.

Stacey, F. D. (2000) Kelvin's age of the earth paradox revisited. *Journal of Geophysical Research: Solid Earth (1978–2012)* **105**(B6), 13155–13158.

Strutt, R. J. (1905) On the radio-active minerals. *Proceedings of the Royal Society of London. Series A, Containing Papers of a Mathematical and Physical Character* **76**(508), 88–101.

Strutt, R. J. (1906) On the distribution of radium in the earth's crust. *Proceedings of the Royal Society of London. Series A, Containing Papers of a Mathematical and Physical Character* **78**(522), 150–153.

Valley, J. W., Reinhard, D. A., Aaron J. Cavosie, A. J., *et al.* (2015) Presidential Address. Nano- and micro-geochronology in Hadean and Archean zircons by atom-probe tomography and SIMS: new tools for old minerals. *American Mineralogist* **100**(7), 1355–1377.

Walcott, C. D. (1893) Geologic time, as indicated by the sedimentary rocks of North America. *The Journal of Geology* **1**(7), 639–676.

Wilde, S.A., Valley, J. W., Peck, W. H., and Graham, C. M. (2001) Evidence from detrital zircons for the existence of continental crust and oceans on the Earth 4.4 Gyr ago. *Nature* **409**(6817), 175–178.

Williams, H. S. (1893) Studies for students: the elements of the geological time-scale. *The Journal of Geology* **1**(3), 283–295.

Zhou, Q., Herd, C. D. K., Yin, Q-Z., *et al.* (2013) Geochronology of the Martian meteorite Zagami revealed by U–Pb ion probe dating of accessory minerals. *Earth and Planetary Science Letters* **374**, 156–163.

CHAPTER 2

Foundations of radioisotopic dating

2.1 INTRODUCTION

Radioactivity, and the geologic clock it provides, is a property of the atomic nucleus. The delineation of the fundamentals of atomic structure occurred over just a couple of decades around the transition from the 19th to 20th century [e.g., *Reed*, 2014, chapter 2]. Understanding the structure of the atom and its constituent particles was without a doubt a first-order advance in our understanding of the nature of matter. Atomic structure provided explanations for the systematic, but often mysterious, behavior of the elements that had been seen over centuries of exploitation of natural ores. While the electrons of an atom primarily control the chemical behavior of an element, the behavior of the nucleus is the foundation of radioisotope geochronology. The importance of this application of nuclear physics is reflected in the fact that the first age determination for a rock using this technique occurred only eight years after the discovery of the first atomic particle, the electron [e.g., *Radash*, 1968]. The basic understanding of the physics of the nucleus provides the tool by which geoscientists over the following century, and continuing today, are able to use naturally occurring isotopic variations in Earth and planetary materials to address a vast range of topics, including questions relating to:

- the origin of the elements in the solar system;
- the chronology and processes involved in planet formation;
- the geologic evolution of Earth and other planets;
- the rates of plate tectonics, basin subsidence, and mountain building;
- absolute ages for the geologic timescale and the evolution of life;
- rates of erosion and modification of the near-surface environment;
- temporal changes in the composition of the atmosphere and the rise of oxygen;
- paleoclimate, paleoecology, and paleogeography.

Geology is in essence the history of the Earth, and for any history dates are absolutely essential. Radioisotope geochronology provides the means to decipher the timescale and rates of all the processes that have created and modified Earth and its surface environment. Understanding the physics of the nucleus and how it leads to stable, and unstable, nuclei provides the background on both the strengths and some of the weaknesses in using radioactive decay as a chronometer.

2.2 THE DELINEATION OF NUCLEAR STRUCTURE

The first big step toward our modern understanding of atomic structure came in 1897 when Joseph (J.J.) Thomson (Fig. 2.1) discovered the electron [*Davis and Falconer*, 2005], an atomic particle characterized by a single negative electrical charge (1.60×10^{-19} coulomb) and a constant mass (9.11×10^{-28}g). Positively charged particles of considerably greater mass were known from the work of Eugen Goldstein in 1886, but these were seen to have different mass to charge ratios depending on what gas was used as a source of the particles. Goldstein's positively charged particles thus could not be characterized as a discrete particle of a constant mass and charge, analogous to the electron. The discovery of both positive and negative charged particles within an atom, however, led to the idea that an electrically neutral atom must be composed of a number of electrons, whose negative charge was balanced by a similar number of positively charged components. Ernest Rutherford in 1911 targeted a beam of high-energy positively charged particles at very thin metal foils and found that in passing through the foil, some particles were strongly deflected from their paths [*Rutherford*, 1911]. Rutherford recognized that these large scattering angles could occur only if the positively charged particles occasionally passed close to an intense positive electric field. This meant that the positive charge in the atoms in the foil must be concentrated into a very small space. Rutherford's experiments showed that all the positive charge in an atom is confined to a nucleus whose diameter is about 10,000 times smaller than that of the atom.

Geochronology and Thermochronology, First Edition. Peter W. Reiners, Richard W. Carlson, Paul R. Renne, Kari M. Cooper, Darryl E. Granger, Noah M. McLean, and Blair Schoene.

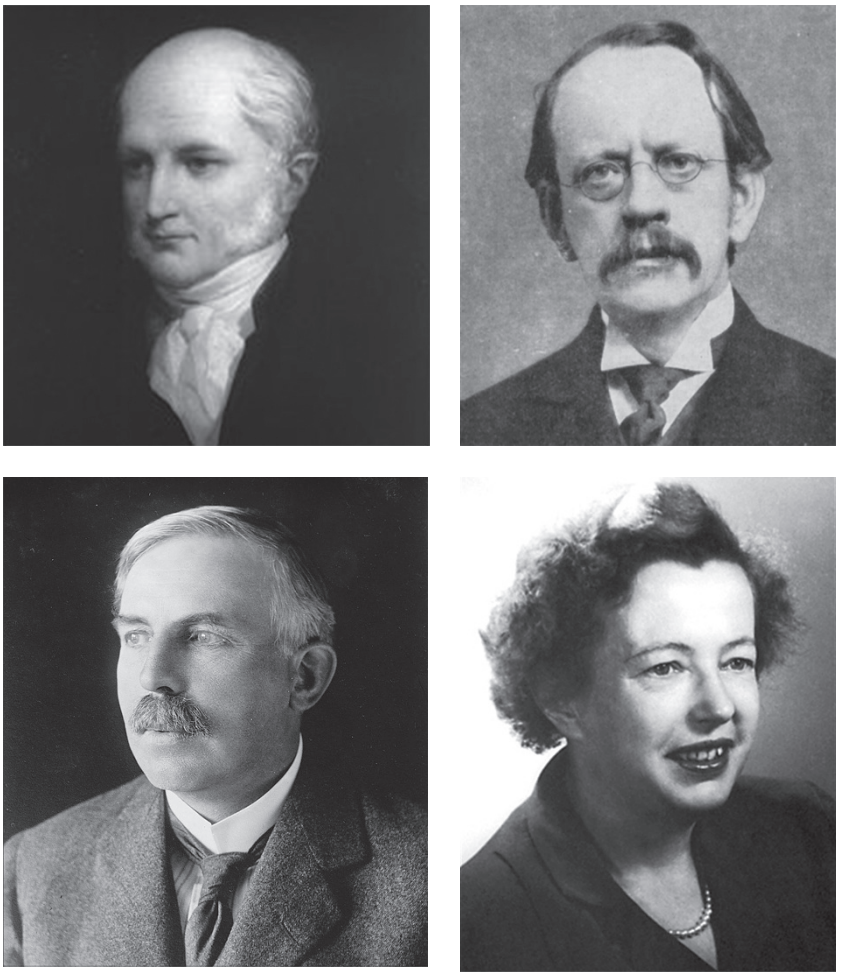

Fig. 2.1. Key players in the delineation of nuclear structure, from left to right: William Prout (By Henry Wyndham Phillips, 1820–1868 (From a miniature by Henry Wyndham Phillips)), Joseph John (J.J.) Thomson (1856–1940), Ernest Rutherford (1871–1937), and Maria Goeppert Mayer (1906–1972).

Rutherford's structural model for an atom thus has a very dense (nuclear densities of 10^{14} g/cm), small ($\sim 10^{-12}$ to 10^{-13} cm), positively charged nucleus surrounded by a diffuse cloud of negatively charged electrons that define an atomic diameter on the order of 10^{-8} cm.

The idea that different elements consist of assemblages of different integer numbers of a fundamental particle dates to well before the identification of the particles that make up the atom. Noting that the mass of many elements are integer multiples of the mass of hydrogen, William Prout in 1815 suggested that different elements reflect different numbers of hydrogen "protyle" in their constituent atoms. The detection of "hydrogen" particles released when nitrogen was bombarded with energetic positively charged particles led Rutherford in 1919 to suggest that the nuclei of all atoms did indeed contain one or more particles that have a single positive charge and a mass similar to that of the hydrogen atom. As this supported Prout's theory, Rutherford named the particle "proton". To achieve charge neutrality, the number of positively charged protons in the nucleus is balanced by the number of negatively charged electrons that orbit the nucleus in a series of "shells" whose electron densities describe shapes that range from the spherical "s" orbitals to the dumbbell shaped lobes of "p" and "d" orbitals, as described in the quantum mechanical model of the atom developed by Niels Bohr. The number of electrons and their residence in specific orbitals is the primary feature that determines the chemical behavior of different elements.

A long-standing argument against Prout's atomic model was that not all elements have masses equal to an integer multiple of the mass of hydrogen. An answer to this valid criticism came with Thomson's discovery in 1913 that neon consists of atoms of two different masses, one with mass ≈ 20 and the other with mass ≈ 22. We now know that neon also contains a low abundance species at mass ≈ 21. Because the different mass neon atoms have essentially identical chemical properties, they must have the same number of electrons and hence the same number of protons in the nucleus. Such atomic species with identical

chemical properties, but different atomic masses, were termed "isotopes" of the element by Frederick Soddy in 1913 after the Greek for "equal (iso) place (topos)," as isotopes had the same chemical properties and hence appeared in the same place in the periodic table. The discovery of isotopes required the presence in the nucleus of another, uncharged, particle of similar mass to a proton. Early experiments with radioactivity had detected electrons (β particles) released by nuclear decay, so an obvious explanation for isotopes was that the nuclei of the two isotopes consisted of different mixtures of protons plus electrons, with the mixture balanced to obtain the correct nuclear charge. Various physical properties, for example the kinetic energy, of β particles were not easily reconciled with a nuclear model of a distributed mixture of electrons and protons. These properties of β particles, however, could be explained if the nuclear electron were tightly bound to a single proton, creating an electrically neutral particle with a mass close to that of a proton. This particle, called a neutron, was eventually found by James Chadwick in 1932, who reported the discovery in a half-page letter to Nature [*Chadwick*, 1932]. The neutron was later shown to have a mass about 0.14% heavier than a proton. The delay in the discovery of the neutron reflects the fact that as an uncharged particle, neutrons cannot be accelerated, and hence separated, by electric fields. In addition, neutrons free from a nucleus decay spontaneously to a proton and electron with a mean lifetime of a bit over 880 s, so they do not stay around long enough to make their detection simple.

Although we now know that both the proton and neutron are composed of mixtures of other particles (proton = 2 up and 1 down quarks; neutron = 1 up and 2 down quarks) [*Thomas and Weise*, 2001], the model of an atom consisting of a nucleus composed of protons plus neutrons, together known as nucleons, surrounded by enough electrons to electrically balance the number of protons explains most of the first order features of all the elements in the periodic table. An individual element is thus defined by the number of protons in the nucleus. The mass (A) of any isotope of that element is the sum of the number of protons (Z) plus neutrons (N) in the nucleus. The atomic mass of an element that contains more than one isotope is then calculated from the sum of the proportion of each isotope times its mass. For example, chlorine consists of a mixture of two isotopes, both containing $Z = 17$ protons, but one with $N = 18$ neutrons (mass = 34.969 g/mol) and the other with $N = 20$ neutrons (mass = 36.966 g/mol). Isotopes conventionally are designated by the integer sum of neutrons and protons in the nucleus (A), so in the case of chlorine, the two isotopes are written as ^{35}Cl and ^{37}Cl. Naturally occurring chlorine is made up of a mixture of 75.76% ^{35}Cl and 24.23% ^{37}Cl, so the atomic mass of Cl is calculated by:

$$\text{Atomic mass (g/mol)} = 0.7576 \times 34.969 \text{ g/mol} + 0.2424 \times 36.966 \text{ g/mol} \quad (2.1)$$

where a mole consists of Avogadro's number (6.0221213×10^{23}) of atoms. At 35.453 g/mol, chlorine is thus one of the elements that appears to argue against Prout's model that every element's mass should be an integer multiple of the mass of hydrogen. This comes about because chlorine has two isotopes, and while the mass of each isotope is nearly an integer multiple of the mass of hydrogen, the mass of the element chlorine is intermediate due to it being a mixture of the two isotopes.

Because electrons are distant from, and hence relatively weakly bound to, the nucleus of their atom, they are free to exchange with nearby atoms. This is the basis of chemical reactions. Given the loosely bound nature of electrons, environmental factors, such as temperature, pressure, and the density and composition of surrounding material, readily influence the chemical reactivity of all elements. As a result, chronological techniques that rely on the chemical reactivity of elements, for instance, optically stimulated luminescence, electron spin resonance (Chapter 10), and amino acid racemization, are sensitive to the environmental conditions that a given sample has experienced. In contrast, the nucleus of an atom is protected from its surroundings by its electron cloud. For this reason, nuclear stability is to a large extent independent of environmental factors, at least up to the point where temperatures or atomic densities approach the very high values found in stellar interiors. The environmental insensitivity of nuclear decay is the primary factor that makes radioisotopic dating so useful for geochronology because the rate of nuclear decay is a constant unaffected by geologic processes. As will be seen in later chapters, the ability of radioactive decay to accurately date various geologic processes does indeed depend on the chemical behavior of the elements involved, but the rate of radioactive decay does not.

2.3 NUCLEAR STABILITY

2.3.1 Nuclear binding energy and the mass defect

An obvious question presented by Rutherford's model of the atom is the nature of the force that keeps the positively charged protons tightly bound in the nucleus rather than allowing them to fly apart due to the electrostatic repulsion of their like charges. That force is referred to as the nuclear binding energy, a residual effect of the strong nuclear force that binds quarks together in the individual nucleons (*Krane*, 1987). The binding energy present in each atom can be calculated through the energy to mass conversion that derives from Einstein's special theory of relativity:

$$E = M \times c^2 \quad (2.2)$$

where E is energy, M is mass, and c is the speed of light. The mass of a proton is 1.67243×10^{-24} g, and the speed of light is 2.9979×10^{10} cm/s. Putting these values into equation (2.2) shows that the mass of a proton corresponds to an energy of 1.503×10^{-3} ergs. An erg is not a large amount of energy, for example, the amount of energy required for a mosquito to take off is estimated at 1 erg. Binding energies are more commonly expressed as electronvolts (eV), which is the energy needed to accelerate one electron through a potential difference of 1 V: 1 eV = 1.602×10^{-12} erg.

On this scale, a proton mass corresponds to an energy of 938 million electronvolts (MeV).

Because the mass of a single atom is so small, the mass of an element or isotope is commonly expressed in units called either unified atomic mass unit (u), or Dalton (Da), that corresponds to the mass of a mole of atoms. Both scales assign the mass of the carbon isotope that has 6 neutrons and 6 protons to exactly 12 Da, or 12 g/mol. On this scale, the mass of a proton is 1.00727 Da, that of a neutron is 1.00866 Da, and an electron is 5.5×10^{-4} Da. Previously, the atomic mass scale was based on the mass of the ^{16}O isotope of oxygen being exactly 16 g/mol. This scale gave rise to the commonly used term AMU, for atomic mass unit. Although use of the ^{12}C scale is now almost universal, acceptance of "u" and "Da" as the abbreviation for the unit has been slow to catch on. As a result, many modern publications still use AMU, but use it with the mass of ^{12}C being defined as exactly 12.000 g/mol.

If the mass of carbon were simply the sum of the masses of its atomic components, then the mass of ^{12}C should be:

$$6 \times 1.00727\,(\text{proton}) + 6 \times 1.00866 \times (\text{neutron}) + 6 \times 0.00055\,(\text{electron}) = 12.0989\,\text{Da}$$

When the protons and neutrons are assembled into an atom, however, the resulting nucleus is more stable than the sum of its parts because it has turned some of the mass of the individual nucleons into nuclear binding energy. The difference in mass between the combination of its atomic constituents and that of the ^{12}C isotope, often called the mass defect, is the energy released by combining these 12 nucleons into a single nucleus. The binding energy of the ^{12}C nucleus is thus:

$$12.0989 - 12.0000\,\text{Da} = 0.0989\,\text{Da which equals } 92.12\,\text{MeV or } 7.68\,\text{MeV per nucleon.}$$

The energy released by fusing enough hydrogen together to make one gram of ^{12}C is thus:

$$92.12\,\text{MeV/atom} \times 6.022 \times 10^{23}\,\text{atoms/mol} \div 12\,\text{g/mol} = 4.62 \times 10^{30}\,\text{eV/g or } 7.4 \times 10^{18}\,\text{ergs/g.}$$

For comparison, typical chemical reactions release of order 10^{13} ergs/g. Fusion reactions occur only at the very high atomic densities and temperatures found in the cores of stars. The much greater energy production from nuclear fusion compared to chemical reactions explains why the Sun can still be emitting so much energy, presently $\sim 4 \times 10^{33}$ erg/s, over 4.5 billion years after its formation. If solar energy were derived solely from chemical reactions, the Sun would have "burned out" long ago.

As shown in Fig. 2.2, binding energy per nucleon peaks between $A = 50$ and $A = 60$, which is in the mass range of iron and nickel. This means that nuclear fusion of light nuclei that result in a product atom near the mass of iron will release energy, whereas fusion of heavier nuclei to produce a product atom significantly higher in mass than iron requires the input of energy. In contrast, nuclear fission, or breaking apart the nucleus of a very heavy element (e.g. uranium) into two like-mass pieces, releases energy because both fission fragments will have nuclei with higher average binding energies than will uranium. The shape of the binding energy versus mass curve in Fig. 2.2 means that if element synthesis were taken to its lowest energy state, the universe would be composed primarily of iron and nickel. While iron and nickel indeed are more abundant in the solar system than elements of similar mass [*Lodders*, 2003], the processing of the matter in the universe is far from complete. Hydrogen and helium are still the most abundant elements in the universe by more than a factor of 10^4 over iron.

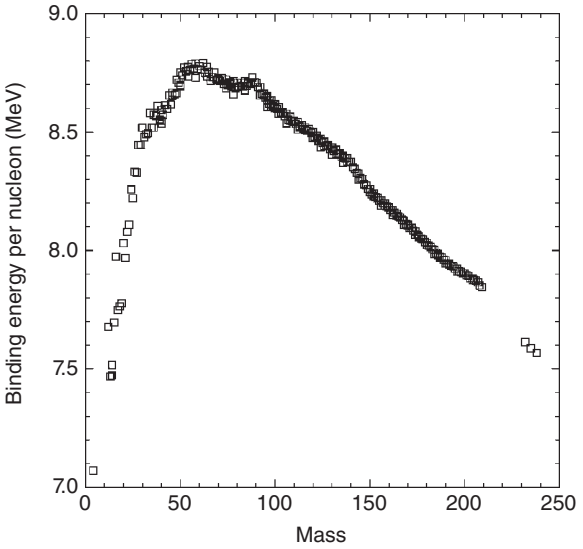

Fig. 2.2. Average binding energy per nucleon for all stable and long-lived isotopes.

2.3.2 The liquid drop model for the nucleus

Nuclear stability is a balance between the strong nuclear force holding the nucleons together and the Coulombic repulsion of the protons due to their positive charge. George Gamow in 1928 first proposed the "liquid drop" model of the nucleus [*Stuewer*, 1997; *Basdevant et al.*, 2005, section 2.2] that treats the nucleus in an analogous way to an incompressible fluid. In this model, an empirical equation with five terms, derived by C.F. von Weizsacker in 1935, that involves only the mass (A) and number of protons (Z) in the nucleus provides a good approximation to nuclear binding energy (E) by taking into account the various forces involved in creating nuclear stability/instability:

$$E = (15.8\,\text{MeV}) \times A - (17.8\,\text{MeV}) \times A^{\frac{2}{3}} - (0.71\,\text{MeV}) \times \frac{Z^2}{A^{\frac{1}{3}}} - (23.7\,\text{MeV}) \times \frac{(A-2Z)^2}{A} \pm \frac{11.2\,\text{MeV}}{A^{1/2}} \tag{2.3}$$

The first three terms in this equation are concerned with the geometry of the "drop". Its volume is proportional to the total number of protons plus neutrons, A, so that its radius is

proportional to $A^{1/3}$, and surface area is proportional to $A^{2/3}$. The first term, the volume term, notes that the total binding energy in the nucleus is proportional to the total number of nucleons, independent of the ratio of protons to neutrons, and reflects the short-range nature of the strong nuclear force. The second term reflects the surface energy of the "drop" and is negative because nucleons at the surface of the nucleus are not surrounded by other nucleons and thus feel less strong nuclear force from surrounding nucleons than those nucleons in the middle of the nucleus. The third term, also negative, reflects the Coulomb repulsion between protons, which will be proportional to the radius of the nucleus.

The last two terms concern the number of protons and neutrons inside the nucleus. The fourth, or asymmetry, term derives from the Pauli exclusion principle that keeps any two nucleons from occupying exactly the same quantum state in an atom. Neutrons and protons occupy different quantum states, so an equal number of protons and neutrons leads to the lowest nuclear energy state because each new nucleon added must be added to a higher energy state than the previous one. The last term, or pairing term, arises because nucleons have spin, and hence angular momentum and magnetic moments. A pair of protons, or neutrons, with opposite spin have more binding energy than a pair with the same spin. The term is written in a way that an even–even number of protons–neutrons adds to the binding energy while an odd–odd number reduces the binding energy in comparison to the baseline odd–even, or even–odd, combinations of neutrons and protons. If A is an odd number, this term is zero. The binding energies calculated as a function of number of protons and neutrons using this equation are shown in Fig. 2.3.

For an atom of any given mass, the liquid drop model equation (2.3) indicates that the binding energy is a parabolic function of the number of neutrons and protons that combine to that mass.

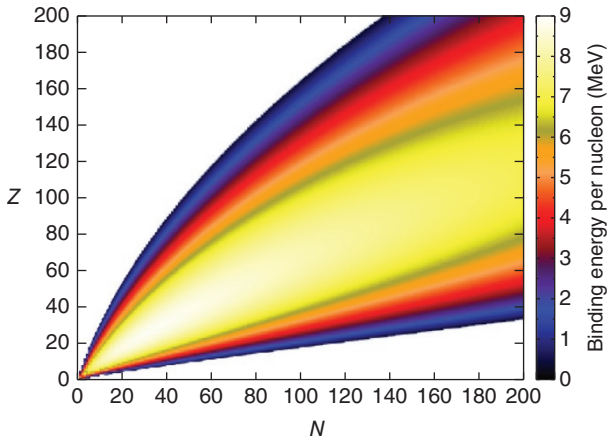

Fig. 2.3. Nuclear binding energies per nucleon as a function of the number of neutrons (N) versus protons (Z) in the nucleus. The binding energies are calculated using the Bethe–Weizsacker equation described above. (Source: Courtesy of Larry Nittler.) (*See insert for color representation of the figure.*)

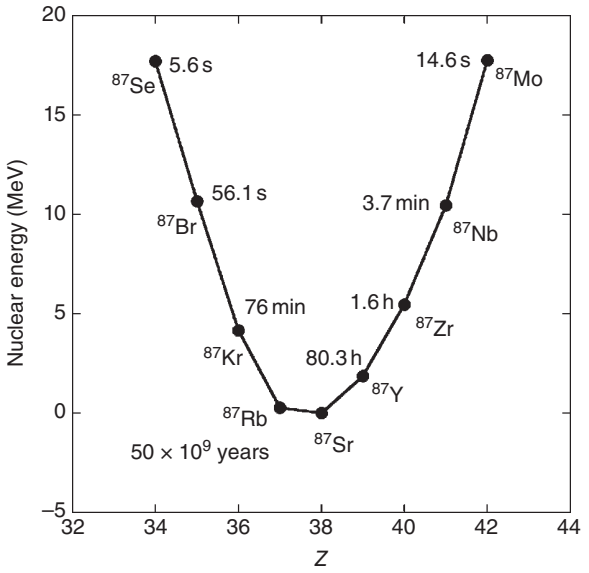

Fig. 2.4. Excess nuclear energy, in MeV, for the addition or subtraction of protons from the stable isotope at mass 87, ^{87}Sr. Each isotope is labeled along the curve with its radioactive decay half-life.

This is illustrated in Fig. 2.4 for $A = 87$. At this mass, the stable isotope is ^{87}Sr that has $Z = 38$ and $N = 49$. Swapping a neutron for a proton, or visa versa, to create an isotope with a different Z than ^{87}Sr increases the energy of the nucleus. As a result, an atom of, for example, $Z = 37$ and $N = 50$ (^{87}Rb) can reduce its nuclear energy by transforming its nucleus through radioactive decay to ^{87}Sr. The total energy released by the radioactive decay is equal to the difference in the nuclear energies of the starting and ending nucleus. In general, the farther an atom gets from the maximum nuclear binding energy for a given mass, the quicker the unstable nucleus decays to a more energetically favorable state, eventually working its way to the stable isotope of that mass, if there is one. As indicated in Fig. 2.3, the steepness of the binding energy parabolas decrease with increasing A, thus creating a broader "well" at the bottom of the parabola that allows for an increasing number of stable isotopes at any given mass as A increases.

The parabolic relationship of nuclear energy versus number of protons for any single mass isotope is the primary control over nuclear stability, but as equation (2.3) indicates, several other factors also contribute to enhancing or reducing nuclear stability. Figure 2.5 shows binding energies for elements with $A < 20$. The rapid increase with mass in binding energy per nucleon is readily apparent in these light elements, but in addition, elements with multiples of mass 4 (2 protons plus 2 neutrons, otherwise known as an α particle or ^{4}He nucleus) show an extra step in binding energy. The extra stability of the mass 4 aggregate reflects the fact that the strong nuclear force extends only over distances comparable to the "nearest neighbor" nucleon, so the grouping of 2 protons and 2 neutrons maximizes the bonding due to the strong nuclear force. The mass 4 nuclear aggregate is so stable that ^{8}Be, composed of two α particles, is unstable and

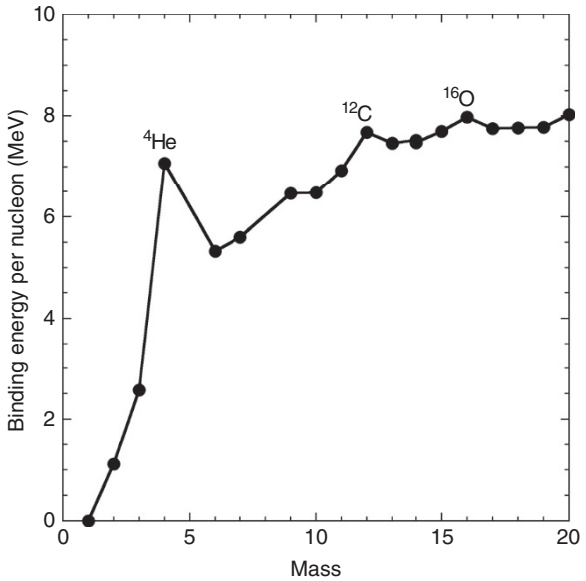

Fig. 2.5. Average binding energy per nucleon versus mass for isotopes of mass 20 or lower.

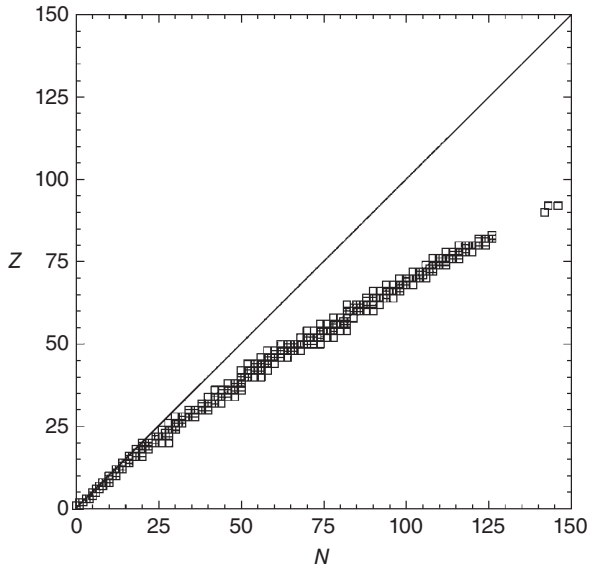

Fig. 2.6. Squares plotted for stable and long-lived isotopes comparing the number of neutrons (*N*) and protons (*Z*) in their nuclei. The line shows where $Z = N$.

decays with a half-life of about 10^{-16} seconds into two ^{4}He nuclei. The extra binding energy per nucleon at mass 8 is not yet sufficient to overwhelm the extra stability of the mass 4 aggregate, whereas it is by mass 12. Consequently, ^{12}C, ^{16}O, ^{20}Ne, ^{24}Mg, ^{28}Si, and ^{32}S are by far the most abundant isotopes in these elements, with all but ^{24}Mg constituting more than 90% of the stable isotopes of each element.

Another factor contributing to the extra stability of the ^{4}He nucleus arises from the pairing term in equation (2.3). Pairing of nucleons with opposite spins results in extra nuclear stability compared to an unpaired nucleon. For this reason, nuclei with an even number of either neutrons or protons are more stable than those with an odd number. As a result, nuclei with an even number of both protons and neutrons are abundant while isotopes with an odd number of both neutrons and protons are rare at any mass above ^{14}N. Of all the stable or long-lived isotopes, 224 are even *Z*, 63 are odd *Z*, and only 9 have both odd-*Z* and odd-*N* and of these, only 3 are found at $A > 50$.

Given the short-range nature of the strong nuclear force, the additional nuclear stability contributed by the grouping of two protons and two neutrons decreases with nuclear mass. Consequently, at higher masses, the Coulomb repulsion of the positive charge of the protons becomes a more important parameter in nuclear stability. Although the asymmetry term in equation (2.3) indicates that an equal number of protons and neutrons leads to the highest binding energy, the extra binding energy contributed by this term is overwhelmed by Coulomb repulsion as *Z* increases. The Coulomb repulsion acts over the whole radius of the nucleus, but is less at greater proton-to-proton distances. Below about $Z = 20$, the strong force dominates and most nuclei have an equal number of protons and neutrons due to the asymmetry term (Fig. 2.6). Above $Z = 20$, the repulsion of protons causes the region of stable nuclei to shift to an increasing ratio of neutrons to protons. This change reflects the need to increase the nuclear radius by adding more neutrons in order to lessen the Coulomb repulsion of the protons. This competition between the strong nuclear binding force and Coulomb repulsion also explains the shape of the nuclear binding energy versus mass relationship at high *Z* shown in Fig. 2.2. Here, the Coulomb repulsion is sufficient to begin to reduce the binding energy per nucleon with the addition of additional protons.

2.3.3 The nuclear shell model

A final parameter that affects nuclear stability is that certain numbers of neutrons and protons provide additional stability to the nucleus. This observation was used by Maria Göppert Mayer in 1948–1950 to suggest a "shell" model for the nucleus [*Mayer*, 1950a, b], analogous to the Bohr electron shell model, where a filled nuclear shell provides additional nuclear stability. The shell model has "magic" numbers of *N* or *Z* of 2, 8, 20, 28, 50, 82, and for neutrons 126. A good example of the consequences of this effect on elements important to geochronology is seen in samarium and neodymium. Both Sm and Nd are even *Z* elements with 7 stable isotopes. Both have isotopes with the magic number of 82 neutrons. As a result, the lightest Nd isotope (^{142}Nd, $Z = 60$, $N = 82$) is the most abundant Nd isotope whereas for most elements in this mass range, the most abundant isotope is in the middle of the mass range for that element. Another example of the extra nuclear stability contributed by the shell model is Sm. Samarium-144 ($Z = 62$, $N = 82$) is stable, yet the next three heavier Sm isotopes are all radioactive. Stability is only reached again at ^{148}Sm.

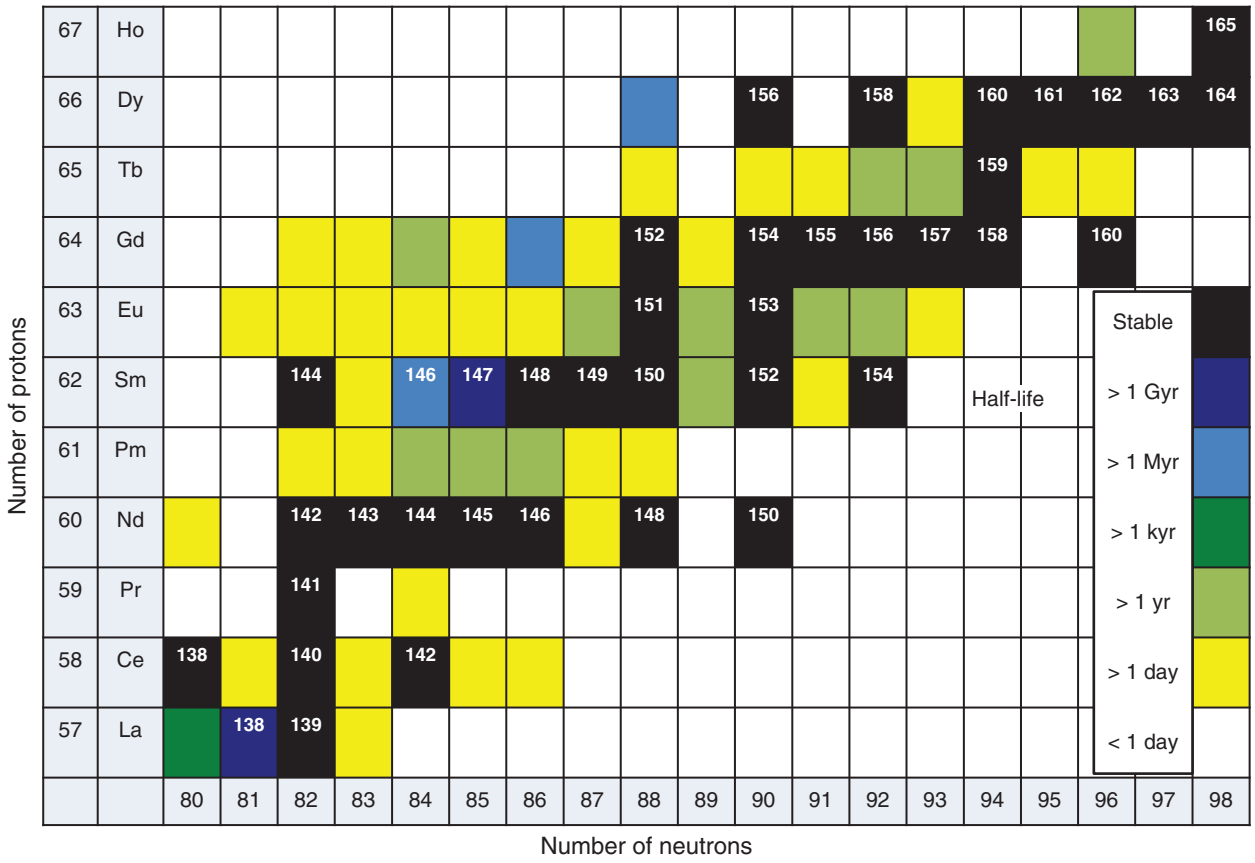

Fig. 2.7. Chart of the nuclides in the mass region of the rare earth elements. Black blocks denote isotopes with half-lives greater than 10^{12} years, dark gray are isotopes with half-lives between 10^6 and 10^{12} years, light gray are isotopes with half-lives of 1 to 10^6 years, and white blocks are isotopes with half-lives of less than a year. Numbers in the blocks give the atomic mass of the isotope. (*See insert for color representation of the figure.*)

2.3.4 Chart of the nuclides

The nuclear stability rules outlined above are well reflected in the chart of the nuclides (Fig. 2.7) that plots N on the x-axis and Z on the y-axis. A stable combination of neutrons and protons in the nucleus creates a "valley of stability", indicated by the black blocks in Fig. 2.7, within the middle of the chart of the nuclides that is coincident with the region of maximum per-nucleon nuclear binding energy shown in Fig. 2.3. For the reason depicted in Fig. 2.4, the presence of too many neutrons or protons leads to nuclei that are unstable with respect to their radioactive decay into nuclei that reside within the valley of stable nuclei. The terminology for various combinations of neutrons and protons shown on the chart of the nuclides includes:

isotopes—atoms of identical Z, but different N and A
isotones—atoms of identical N, but different Z and A
isobars—atoms of identical A, but different Z and N.

On the chart of the nuclides, isotopes define rows, isotones define columns, and isobars plot with a slope of $-45°$.

2.4 RADIOACTIVE DECAY

As shown in Fig. 2.4, an atom with an unstable number of neutrons and protons can reach a lower nuclear energy state by transforming the nucleus into a more stable combination of nucleons in the process known as radioactive decay. In radioactive decay, the radioactive isotope is often referred to as the parent isotope whereas the decay product is the daughter isotope. Depending on the mass of the radioactive nucleus, and whether it lies to the neutron-rich or neutron-poor side of the valley of nuclear stability, its transformation into a stable isotope can take many forms.

2.4.1 Fission

Given the slope of the energy per nucleon versus mass curve shown in Fig. 2.2, all nuclei heavier than about mass 100 can reach lower nuclear energy states by breaking into two fragments. This form of radioactive decay, known as fission, occurs at measureable rates only in atoms with $A > 230$. What stops lighter elements from fissioning is the need for the two fragments to

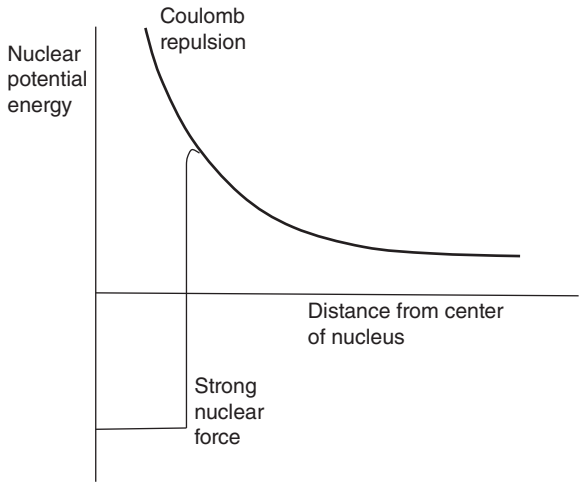

Fig. 2.8. Schematic representation of the energy balance of an atomic nucleus. Coulomb repulsion of two positively charged particles rises in proportion to the inverse of the separation distance squared, but at some distance, the attractive strong nuclear force begins to overwhelm the Coulomb repulsion. (Source: Adapted from *Friedlander et al.* [1981]. Reproduced with permission of John Wiley & Sons.)

overcome the energy barrier created by the strong nuclear force that would allow the two parts of the fissioning nucleus to get far enough apart so that Coulomb repulsive forces become dominant.

For a nucleus to be stable, one can envision a plot of nuclear potential energy versus distance from the center of the atom to look something like the curve shown in Fig. 2.8 [*Friedlander et al.*, 1981]. Two positively charged particles being brought together would encounter increasing Coulomb repulsion as their separation decreases, but at some point, the strong nuclear force must overcome the Coulomb repulsion so that the two particles can bind to form a stable nucleus. Reversing this process in order to fission, the two pieces of the nucleus would have to have enough energy to escape from the energy well created by the strong nuclear force. Given the charge and radii of two halves of a ^{238}U nucleus, the energy needed to penetrate this barrier is nearly 200 MeV. The energy released during ^{238}U fission is of order 180 MeV, so it is only through quantum mechanical effects that a uranium nucleus can occasionally "tunnel" through the energy barrier to fission. As the mass of the nucleus declines, both the Coulomb barrier and the energy released in fission decline, but the Coulomb energy declines more slowly, leading to decreasing probability of fission in lighter nuclei; of the naturally occurring elements, only ^{238}U and ^{244}Pu fission at measureable rates. Fission generally does not split the nucleus exactly in half, but instead into two daughters of unequal mass. For example, ^{238}U fission produces daughter nuclei ranging from ^{66}Mn to ^{172}Ho, but with two peaks in abundance of the daughter isotopes from $A = 87$ to 104 and $A = 132$ to 149. Because of the high neutron to proton ratio in nuclei of high mass, most of the daughter isotopes produced by fission lie to the neutron-rich side of the valley of stability. As a result, most of the products of fission are themselves radioactive isotopes.

One way to accelerate the rate of fission is to add energy to a nucleus, for example by allowing it to capture a neutron. Neutrons can penetrate into the nucleus because they have no charge, and hence no Coulomb repulsion. Laboratory neutron-induced fission of uranium was first accomplished by Enrico Fermi in 1934, but Fermi misinterpreted the product of neutron irradiation of uranium as a heavier element. Similar experiments performed by Otto Hahn, Lise Meitner, Otto Frisch, and Fritz Strassmann proved in 1938 that one of the products of neutron irradiation of uranium was barium, an element of roughly half the mass of uranium (http://www.chemheritage.org/discover/online-resources/chemistry-in-history/themes/atomic-and-nuclear-structure/hahn-meitner-strassman.aspx).

Besides the two heavy nuclei, fission often releases α particles and free neutrons. The neutrons can then go on to induce fission in nearby uranium atoms. If the density of uranium is sufficient, a "critical mass" is achieved when the neutrons released from a fission event can induce enough additional U atoms to fission, releasing more neutrons, that the reaction becomes self-sustaining. This is the operating principle of both the fission bomb and most nuclear power plants. Nature, however, was the first to perform this experiment when at least one naturally occurring uranium deposit, Oklo in Gabon, Africa reached a sufficient uranium density to sustain a natural fission reactor. This natural reactor was in operation 1.7 billion years ago and likely ran for a few hundred thousand years. The Oklo natural reactor was discovered when it was found that the U from this mine was deficient in ^{235}U compared to most natural U, as the ^{235}U was consumed by the sustained fission [*Meshik*, 2005].

Applications of fission in geochronology include the production of xenon from the fission of U and Pu (Chapter 14), and the damage to crystals that results when the energetic fission particles rip through a crystal lattice (Chapter 10).

2.4.2 Alpha-decay

Rather than splitting into two near equal size fragments, another way for heavy elements to gain nuclear binding energy is to eject an α particle. This is a preferred decay mechanism because of the high binding energy per nucleon of the ^{4}He nucleus. The declining binding energy per nucleon versus mass at $A > 60$ means that the combined binding energy of the α particle and any nucleus with $A > 140$ that underwent α–decay would be higher per nucleon than of the predecay nuclei. As with fission, however, ejection of an α particle from the nucleus requires overcoming the strong nuclear force holding the two particles together, which leads α–decay to be a less common means of decay than expected from nuclear binding energy considerations alone. The Coulomb repulsion of a +2 charged α particle, however, is always < 13 MeV and generally ~5 MeV, compared to the > 100 MeV energies associated with fission.

The ejection of an α particle causes Z to decrease by 2 and A by 4; for example, ^{147}Sm α–decays to form ^{143}Nd. Although more common than fission, in the naturally occurring radioactive isotopes, α–decay occurs only in ^{146}Sm (Chapter 14), ^{147}Sm (Chapter 6), ^{190}Pt (Chapter 7) and Th and U (Chapter 8) and their decay chain nuclides (Chapter 12). Besides the daughter isotopes produced by α-decay, the abundance of the α particle itself, which becomes ^{4}He, is a useful chronometer (Chapter 11).

2.4.3 Beta-decay

Unlike fission and α–decay that involve interaction of the strong nuclear force and the Coulomb repulsion of two positively charged particles, β–decay reflects the transformation of a single nucleon, with the ejection of either a positive or negatively charged electron. For isotopes on the neutron-rich side of the valley of nuclear stability, β–decay involves the emission of a nuclear electron, reflecting the conversion of a neutron into a proton. This form of β–decay increases Z by 1 while reducing N by 1, with no change to A. For example, ^{87}Rb β-decays to ^{87}Sr.

An analogous decay mechanism occurs to nuclei on the proton-rich side of the valley of stability, but involves the ejection of a positron, the antimatter counterpart to the electron. Positrons have the mass of an electron, but a positive charge. Positron decay transforms a proton into a neutron and thus increases N by 1, decreases Z by 1, but keeps A constant. Both β–decay and positron-decay produce isobars of the starting atom. β-decay is the basis of many radioactive systems used in geochronology, including ^{10}Be, ^{26}Al, ^{53}Mn, ^{60}Fe, ^{87}Rb, ^{107}Pd, ^{129}I, ^{176}Lu, ^{182}Hf, ^{187}Re (Chapters 6, 7, 13, 14) and several of the members of the U and Th decay chains (Chapter 12).

2.4.4 Electron capture

A final means of radioactive decay involves the capture of an inner electron in the atom by the nucleus, transforming a proton into a neutron. Electron capture, much like positron decay, thus decreases Z by 1, increases N by 1, but leaves A unchanged. Unlike all other forms of radioactive decay, electron capture does not release a charged particle, only the energetic photon of a gamma ray if the decay occurs to an excited nuclear state of the daughter nucleus. The removal of an electron from the electron shell of the element, however, often results in emission of an X-ray photon as the atom moves an electron from an outer shell to fill the electronic state vacated by the electron consumed by the nucleus. The geochronologically most useful electron capture decay is the transformation of ^{40}K to ^{40}Ar (Chapter 9).

2.4.5 Branching decay

For a small number of isobars, the shape of the nuclear energy versus Z parabola (e.g., Fig. 2.4) allows the isotope to gain nuclear stability through more than one decay path. A good example is ^{40}K ($Z = 19$, $N = 21$), whose nuclear stability is relatively low because it has an odd number of both neutrons and protons. Figure 2.9 shows the nuclear energy parabola for isobars of $A = 40$. In this mass range, ^{40}Ca (Z = 20, $N = 20$) is unusually stable because it has a magic number of both neutrons and protons. This feature leads the ^{40}Ca nucleus to be more stable than ^{40}K. The nucleus of ^{40}K can therefore improve its nuclear stability by decaying either to ^{40}Ar or to ^{40}Ca. Consequently, 88.8% of ^{40}K decays via β-decay to ^{40}Ca and the remainder decays to ^{40}Ar, primarily by electron capture. For similar reasons ^{138}La ($Z = 57$, $N = 81$—an odd–odd nuclei) undergoes branched decay to both ^{138}Ce ($Z = 58$, $N = 80$) and ^{138}Ba ($Z = 56$, $N = 82$), and ^{176}Lu ($Z = 71$, $N = 105$—another odd–odd nuclei) decays to both ^{176}Hf ($Z = 72$, $N = 104$) and ^{176}Yb ($Z = 70$, $N = 106$).

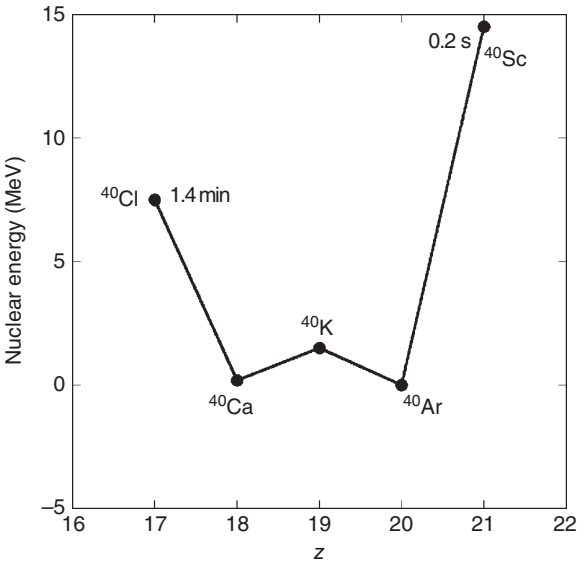

Fig. 2.9. Nuclear potential energy diagram for isobars of mass 40. Because ^{40}Ca consists of a magic number (20) of both neutrons and protons, its nuclear stability is increased enough so that it is more stable than its ^{40}K isobar. As a result, radioactive ^{40}K can decay to either ^{40}Ca or ^{40}Ar and gain nuclear stability. The decay times (half-life) of the unstable ^{40}Cl and ^{40}Sc are shown.

2.4.6 The energy of decay

Radioactivity was first discovered because the high energy of the emitted particles led them to create noticeable reactions in either photographic film or when passing through low-vacuum chambers where they could ionize the gas present, creating electric currents in the process [e.g., *L'annunziata*, 2007]. Conservation of energy requires that the energy of nuclear decay must exactly equal the total binding energy difference between the parent and daughter nuclei. In both fission and α–decay, most of this energy is transformed into the kinetic energy of the particles produced.

During nuclear fission, the energy released by splitting the nucleus in two is mostly transformed into the kinetic energy of the two fission particles, so in a ^{238}U fission event, the two fragments fly apart with a total kinetic energy approaching 180 MeV. If the fissioning U atom is contained within a crystal lattice, the energetic fission particles impact neighboring atoms, stripping at

least some of their electrons, breaking chemical bonds in the process, and displacing atoms from their sites in the crystal lattice. The result is a path of crystal damage about 5 nm wide and 10–15 μm long. These damage paths, called fission tracks, can be enlarged using chemical etching so that they can be observed in an optical microscope. Counting the density of the fission tracks in comparison to the amount of uranium in a crystal is the basis of the technique of fission track geochronology, discussed in Chapter 10.

During α–decay, the total energy of the decay also is partitioned into the two fragments according to their mass, and because momentum is conserved during the decay:

$$Vn = (M\alpha/Mn) \times V\alpha \tag{2.4}$$

V and M are the velocity and mass, respectively of the α particle and nucleus (n) that emitted the α particle. For ^{238}U, which decays to ^{234}Th by α emission, this means that the recoil velocity of the decaying ^{234}Th nuclei is 1.7% (4/234) of that of the emitted α particle.

Neither the α particle nor the recoiling residual nucleus cause enough damage to a crystal lattice to make a track that can be seen by optical microscopy after chemical etching, nevertheless, the energetic particles do damage the crystal lattice. Even at relatively low radiation doses, the crystal damage can be sufficient to affect the diffusion rates of elements through the lattice. At high radiation doses, the damage can be so severe that the crystal structure is destroyed, leading to an amorphous state called "metamict." Alpha-particle passage through some plastics, however, does create damage paths that can be chemically etched to be visible under optical microscopes. This effect can be a useful way to map the abundance of α particle emitters in a material [*Enge*, 1980].

Beta- and positron-decay result in the emission of an electron or positron whose energy is highly variable. Because energy should be conserved during a radioactive decay, the variable energy of emitted β particles and positrons indicates that at least some of the energy of β–decay must be distributed to other emissions. The most easily detected of these are gamma rays. Gamma rays due to β–decay arise from one of two mechanisms. First, when a positron encounters an electron, the two combine and annihilate one another to produce two gamma rays of energy equivalent to the rest mass of the electron. Using equation (2.2) and an electron mass of 9.11×10^{-28} g, each of the two gamma rays derived from positron-electron annihilation will produce a gamma ray of 0.51 MeV. Second, gamma rays of different, but discrete, energies are emitted when the β–decay leads to a daughter nucleus that is not in its ground energy state. Much like electron orbitals of differing energy give rise to the emission spectra of elements, quantum mechanical models for the nucleus describe the presence of discrete energy levels within the nucleus. Figure 2.10 shows how the decay to different excited nuclear states of a daughter isotope can lead to the emission of β particles and gamma rays of differing energies.

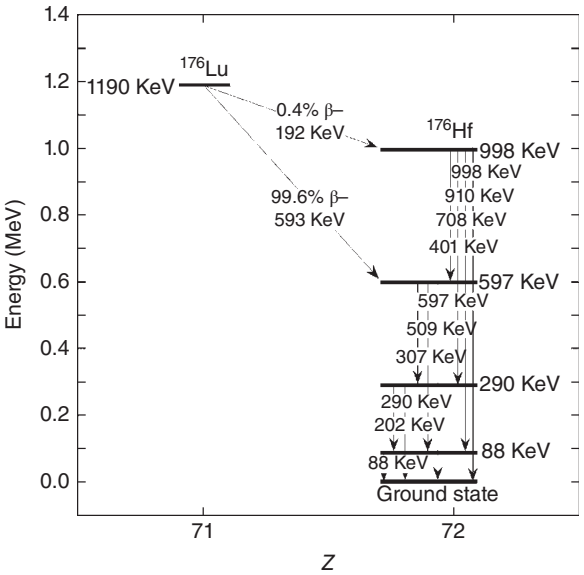

Fig. 2.10. Nuclear potential energy levels tracing one path for the β–decay of ^{176}Lu to ^{176}Hf. This decay primarily (99.6% of the time) occurs with the emission of a 593 KeV maximum energy electron, but occasionally occurs through a much lower maximum energy (192 KeV) electron emission. Both decay paths leave the ^{176}Hf daughter isotope in an excited nuclear state. To reach the ground state, the ^{176}Hf can then emit a number of different gamma rays as the nucleus moves through various excited states to its ground-state energy level. The gamma rays are of the discrete energy indicated by the difference in energy levels of the excited nuclear states. The energies listed for the β particles are maxima because a fraction of the decay energy is partitioned between electron and neutrino during β–decay.

In general, the electrons/positrons emitted by β–decay do not have discrete energies, but instead show a smooth distribution of energies with an average energy of about one-third the maximum energy (Fig. 2.11). Although apparently violating conservation of energy laws, the energy distribution of β particles instead reflects the partitioning of the decay energy between the β particle and another particle, the neutrino. With no charge and a very small mass, currently estimated at less than 0.3 eV, neutrinos interact with matter only through the weak nuclear force, allowing them to pass through matter largely unimpeded. As a result, their detection is extremely difficult, so their discovery was delayed until 1956. The type of neutrino (electron antineutrino) emitted in naturally occurring β–decay has been given the name "geoneutrino." Geoneutrinos are currently being detected using large (kiloton) liquid scintillation chambers buried underground to eliminate background sources of ionizing radiation [*Bellini et al.*, 2010]. Because a neutrino emitted by a decaying U or Th atom anywhere in Earth has a finite probability of reaching the detector, quantifying the rate of geoneutrino emission offers the potential to determine both the average abundance of U and Th in all of the Earth's interior and, at least to low spatial resolution, the distribution of these elements within Earth's interior [e.g., *Sramek et al.*, 2013].

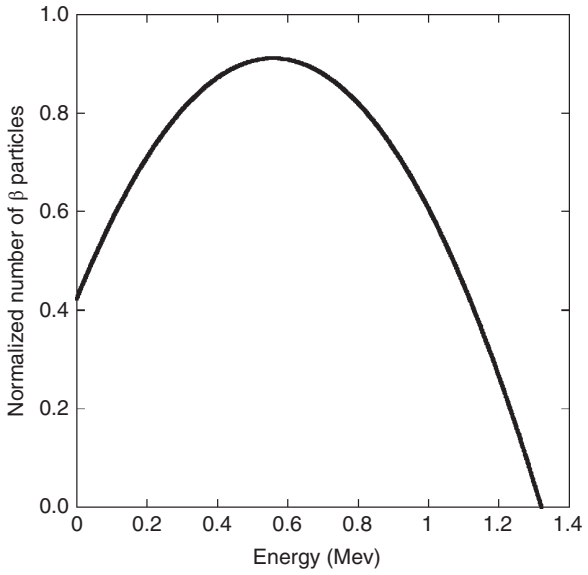

Fig. 2.11. Energy distribution of the β-particles emitted during the decay of ^{40}K. The decay has a maximum energy of 1.31 MeV, but the β-particles show a continuous distribution of energies peaking near 0.6 MeV. The energy difference is contained in the neutrino emitted by this decay. (Source: Adapted from *Cross et al.* [1983].)

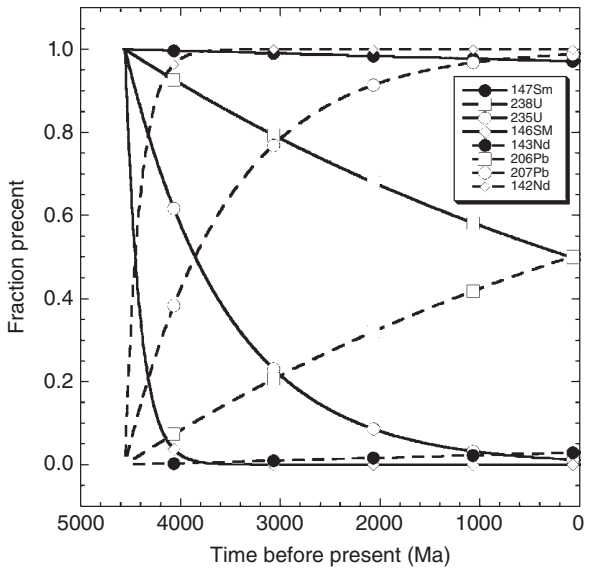

Fig. 2.12. Changing relative abundance of parent (solid curves) and daughter (dashed curves) isotopes of several radioactive isotope systems used in geochronology normalized to their abundance at the time of Earth formation, 4.567 Ga (billion years ago). The lines for the daughter isotopes show only the amount of ingrowth created by the decay of the parent isotope, which is set at zero at Earth formation in this figure. Over the age of the Earth, the abundance of ^{238}U has decreased to 49% of its original abundance because the half-life of ^{238}U (4.47 Ga) is similar to the age of the Earth. In contrast, only a small fraction of radioactive isotopes with substantially longer half-lives have decayed over Earth history. For example, only about 3% of ^{147}Sm ($T_{1/2}$ = 106 Ga) has decayed over Earth history. For those isotopes with half-lives substantially shorter than the age of the Earth, most, or all, of the isotope has decayed away over Earth history. In the case of ^{235}U ($T_{1/2}$ = 0.7 Ga), only a bit over 1% of the original abundance remains, while ^{146}Sm ($T_{1/2}$ = 0.1 Ga) essentially became extinct prior to about 4.0 Ga.

2.4.7 The equations of radioactive decay

The probability that a radioactive isotope will undergo decay over any time interval is proportional to the number of atoms of the radioactive isotope present:

$$\frac{dN}{dT} = -\lambda N \tag{2.5}$$

where N is the number of atoms of the radioactive species, t is time, and λ is the decay constant for the radioactive isotope. The decay constant for a radioactive element describes its rate of decay. Many decay constants are determined by counting the number of energetic particles released by the decay of the radioactive element over some time interval, creating curves for the change in activity with time like those shown in Fig. 2.12. For radioactive isotopes with half-lives in the range of many millions or billions of years, the rate of change of radioactive decay is small over the months to years of a typical counting experiment. For these long-lived radioactive isotopes, an alternative approach for determining a decay constant is to use the radiometric system to measure an age for a rock, and then compare that age with the age determined by some other radiometric system for which the decay constant is better known. This is known as a "geologically determined" decay constant. As will be made clear in later chapters, the decay constant is a measured parameter, subject to all the usual uncertainties of any measurement. The accuracy and precision of the decay constant thus directly impacts the accuracy and precision of any age determined using radioactive decay systems, particularly when comparing ages measured by different radiometric systems. With any single radioactive parent, however, the accuracy of the decay constant affects only the accuracy of the age determined, not the relative age difference between two rocks dated using the same radiometric system.

Integrating equation (2.5) in the form:

$$\frac{dN}{N} = -\lambda dt \tag{2.6}$$

provides the number of atoms of the radioactive species present at any time in proportion to the starting quantity of the isotope:

$$\ln(N) = -\lambda t + C \tag{2.7}$$

where C is a constant. Before any decay has occurred, N is equal to the number of atoms present when $t = 0$ (N_0), so

$$C = \ln(N_0) \tag{2.8}$$

Equation (2.6) can thus be rewritten as:

$$\ln(N/N_0) = -\lambda t \tag{2.9}$$

which is equivalent to:

$$N = N_0 e^{-\lambda t} \tag{2.10}$$

The rate of radioactive decay also is commonly expressed as "half-life", or the time needed in order for half of the starting number of atoms to experience radioactive decay. In equation form, the half-life is thus when $N/N_0 = 0.5$ so the half-life ($T_{1/2}$) is related to the decay constant by the equation:

$$T_{\frac{1}{2}} = \frac{\ln(2)}{\lambda} \tag{2.11}$$

Another useful parameter in radioactive decay is the mean-life (τ) that represents the average life expectancy of an atom of a radioactive species. The mean-life is defined as:

$$\tau = \frac{-1}{N_0}\int_{t=0}^{t=\infty} t\,\mathrm{d}N \tag{2.12}$$

Using equation (2.6), equation (2.12) can be rewritten as:

$$\tau = \frac{1}{N_0}\int_0^{\infty} \lambda N t\,\mathrm{d}t \tag{2.13}$$

and then using equation (2.10), (2.13) is rewritten as:

$$\tau = \lambda\int_0^{\infty} t e^{-\lambda t}\,\mathrm{d}t \tag{2.14}$$

whose solution is:

$$\tau = -\left[\frac{\lambda t + 1}{\lambda} e^{-\lambda t}\right]\frac{\infty}{0} \tag{2.15}$$

so the mean life simply is equal to the inverse of the decay constant, or:

$$\tau = \frac{1}{\lambda} \tag{2.16}$$

The amount of daughter isotope produced by radioactive decay is described simply as:

$$D = N_0 - N \tag{2.17}$$

Where the number of atoms of daughter isotope (D) produced by radioactive decay is simply the difference in the number of atoms of the parent isotope between some starting time ($t = 0$, N_0) and some later time t (N). Using equation (2.10), (2.17) can be rewritten as:

$$D = N_0 - N_0 e^{-\lambda t} \quad \text{or} \quad N_0\left(1 - e^{-\lambda t}\right) \tag{2.18}$$

These equations assume that no atoms of the daughter isotope were present at $t = 0$, but this is not always true. If some number of daughter atoms (D_0) were present at $t = 0$, then equation (2.18) becomes:

$$D = D_0 + N_0\left(1 - e^{-\lambda t}\right) \tag{2.19}$$

Because one often does not know the number of atoms of the radioactive species present at $t = 0$, equation (2.19) can be expressed using parameters that can be measured by using equation (2.10) to substitute N for N_0. Equation (2.19) then becomes:

$$D = D_0 + \frac{N}{e^{-\lambda t}}\left(1 - e^{-\lambda t}\right) \tag{2.20}$$

which can be rewritten as:

$$D = D_0 + N\left(e^{\lambda t} - 1\right) \tag{2.21}$$

When the daughter element has more than one stable isotope, because isotope ratios can be measured much more precisely than the absolute abundance of any given isotope, equation (2.21) is rewritten normalizing to one of the stable isotopes of the daughter element:

$$\frac{D_r}{D_s} = \left(\frac{D_r}{D_s}\right) + \frac{P}{D_s}\left(e^{\lambda t} - 1\right) \tag{2.22}$$

where D_r is the radiogenic isotope of the daughter element, D_s is a stable isotope of that element, and P is the radioactive parent isotope. $(D_r/D_s)_0$ is the isotope ratio of the daughter element at $t = 0$. For example, in the ^{147}Sm–^{143}Nd system, D_r is ^{143}Nd, the decay product of ^{147}Sm, and D_s is ^{144}Nd, so for this system, equation (2.22) is:

$$\frac{^{143}\mathrm{Nd}}{^{144}\mathrm{Nd}} = \left(\frac{^{143}\mathrm{Nd}}{^{144}\mathrm{Nd}}\right)_0 + \frac{^{147}\mathrm{Sm}}{^{144}\mathrm{Nd}}\left(e^{\lambda t} - 1\right) \tag{2.23}$$

This equation describes a straight line on a plot of the two parameters that can be measured in a sample, ^{143}Nd/^{144}Nd (y) versus ^{147}Sm/^{144}Nd (x). On such a plot (Fig. 2.13), a series of samples that formed at the same time with the same initial isotopic composition, but with different parent/daughter elemental ratios, for example different minerals that crystallized from the same magma, will define a line whose intercept with the y-axis defines the daughter isotopic composition of the magma at the time the crystals formed, and whose slope is equal to $e^{\lambda t} - 1$. Solving for "t", the time when the minerals crystallized, then gives:

$$t = \frac{\ln(\text{slope} + 1)}{\lambda} \tag{2.24}$$

This line is called an *isochron*. The isochron method is a critical approach for geochronology as it simultaneously allows determination of both the age and initial isotopic composition of the daughter element of a sample. Applications of the isochron method are described in many of the following chapters, particularly Chapters 4, 6, 7 and 14.

The equations above describe the situation where a radioactive isotope decays to a stable isotope. The U and Th decay chains, however, involve a series of radioactive isotopes that decay to other radioactive isotopes. In this case, equation (2.5) becomes:

$$\frac{\mathrm{d}N_b}{\mathrm{d}t} = \lambda_a N_a - \lambda_b N_b \tag{2.25}$$

where N_a is the first radioactive element in the chain that decays to N_b with a decay constant of λ_a, but N_b also is radioactive with a

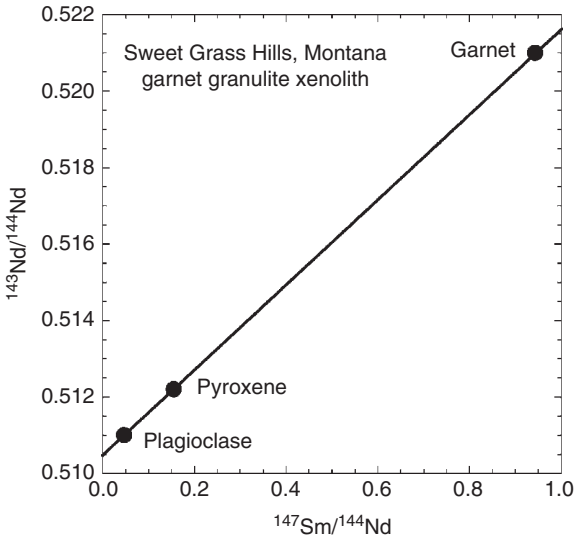

Fig. 2.13. Sm–Nd isochron diagram for minerals separated from a garnet granulite lower crustal xenolith from the Sweet Grass Hills, Montana. The three minerals in the rock formed with a relatively wide range in Sm/Nd ratios, and, as a result of radioactive decay of ^{147}Sm, now display a wide range in ^{143}Nd/^{144}Nd ratios. The three points define a line, called an isochron, that has a slope equal to 0.01115, which corresponds to an age of 1696 ± 6 Ma. The isochron intercepts the *y*-axis at ^{143}Nd/^{144}Nd = 0.51046 ± 0.00002, which corresponds to the isotopic composition of the Nd incorporated into these minerals when this rock formed. (Source: data from *Irving et al*. [1997].)

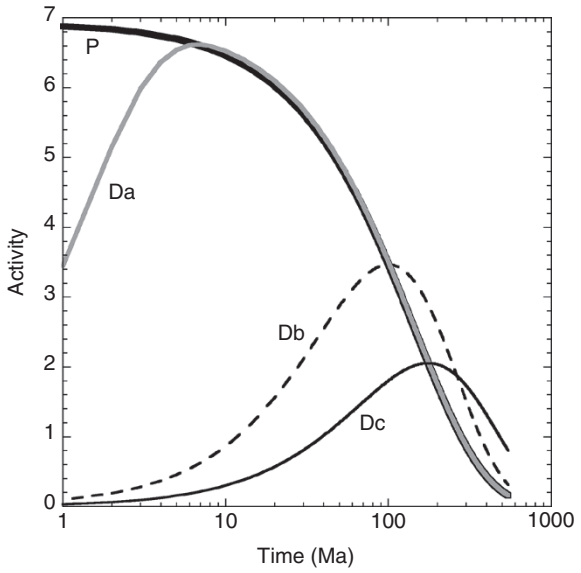

Fig. 2.14. Change in radioactivity with time for an initially pure radioactive parent isotope (*P*) with 10^8 years half-life. The parent isotope decays away at an exponential rate determined by its half-life (thick black line), but as it decays, it produces a daughter isotope that is itself radioactive. If that daughter isotope has a half-life much shorter than the parent, for example D_a (gray line) with a half-life of 10^6 years, the activity of that daughter will initially increase as the abundance of D_a increases due to production from the decay of *P*. Eventually, the decay rate of the daughter will equal the production rate and so its activity will stay equal to that of the parent in the condition called secular equilibrium. A similar situation is reached should the daughter isotope have a decay rate only somewhat quicker than the parent (D_b, with half-life of 10^7 years), but when the state of transient equilibrium is reached, the activity of the daughter will be higher than that of the parent as described by equation (2.30). When the daughter has a longer half-life than the parent (D_c with 1.5×10^8 years half-life), the ratio of activity of daughter to parent will continue to increase throughout the lifetime of the parent.

decay constant of λ_b. The equation accounts for the ingrowth of N_b due to production by the decay of N_a, but also the loss of N_b due to its radioactive decay to an element further down the decay chain. The solution to this differential equation is:

$$N_b = \frac{\lambda_a}{\lambda_b - \lambda_a} N_a^0 \left(e^{-\lambda_a t} - e^{-\lambda_b t}\right) + N_b^0 e^{-\lambda_b t} \tag{2.26}$$

where N_a^0 and N_b^0 are the abundances of N_a and N_b at $t = 0$. The first term in the equation describes the production rate of N_b while the second tracks the decay of whatever N_b was present at $t = 0$.

If the half-life of the parent isotope is considerably longer than the half-life of the daughter isotope (e.g. $\lambda_a < \lambda_b$), after a sufficient time, $e^{-\lambda bt}$ becomes small relative to $e^{-\lambda at}$. In this case, equation (2.26) reduces to:

$$N_b = \frac{\lambda_a}{\lambda_b - \lambda_a} N_a^0 e^{-\lambda_a t} \tag{2.27}$$

which, because $N_a = N_a^0 e^{-\lambda at}$, can be further reduced to:

$$\frac{N_b}{N_a} = \frac{\lambda_a}{\lambda_b - \lambda_a} \tag{2.28}$$

This is a state known as *transient equilibrium*. When using radioactive counting methods to determine the abundance of a radioactive isotope, the number of radioactive decays that occur over some time interval is called the *activity* of the radioactive isotope. The activity, written as $[N_a]$, is equal to the abundance of the radioactive isotope times its decay constant, or:

$$[N_a] = \lambda_a N_a \tag{2.29}$$

Using this definition of activity, equation (2.28) can be rewritten as:

$$[N_a] = [N_b] - N_b \lambda_a \tag{2.30}$$

In an initially pure sample of the parent isotope (N_a), the activity of the daughter isotope (N_b) starts at zero, but grows in rapidly until it exceeds the activity of the parent, but then, when transient equilibrium is reached, the activity of N_b declines at a rate that follows the activity decline of the parent, though offset to higher activity by an amount proportional to the difference of the decay constants of elements *a* and *b* (Fig. 2.14).

In the special case where the half-life of the daughter isotope is much shorter than that of the parent isotope ($\lambda_a << \lambda_b$), which

is true for many isotopes in the U and Th decay chains (Chapter 12), equation (2.30) reduces to:

$$[N_a] = [N_b] \tag{2.31}$$

which describes a state known as *secular equilibrium*. In secular equilibrium, the activity of the daughter isotope is the same as that of the parent isotope. Secular equilibrium is reached after several half-lives of the daughter isotope have passed (Fig. 2.14).

2.5 NUCLEOSYNTHESIS AND ELEMENT ABUNDANCES IN THE SOLAR SYSTEM

2.5.1 Stellar nucleosynthesis

The nuclear stability rules described above provide a framework for understanding how elements are made and how our solar system ended up with the mixture of elements it contains [*Truran and Heger*, 2003]. Starting with a universe that had only hydrogen and helium, gravitational attraction of "clumps" of this gas, if in sufficient quantity, led to the formation of the first stars. If sufficiently massive, the gravitational force pulling the hydrogen in the star towards the center of mass can create pressures and temperatures sufficiently high to strip electrons from atomic nuclei, and provide enough energy to the resulting bare nuclei to overcome their Coulomb repulsion so that the nuclei can begin to interact with one another. At temperatures of about 14 million degrees kelvin, hydrogen fusion can take place. Once nuclear fusion reactions start, the energy released is sufficient to halt the gravitational collapse of the star. This creates a stable balance between gravity, which causes the star to contract, and the energy released by fusion, which drives the star to expand. At this point, the star is luminous and begins a relatively stable phase, becoming what is known as a "main sequence" star. The Sun is a main sequence star about half-way through its lifetime of stable nucleosynthesis.

The first stage of element synthesis transforms hydrogen into helium. In relatively low mass stars like the Sun, this takes place through proton–proton chain reactions that can occur in up to about the inner third of the star's radius. This sequence of reactions goes as follows:

$$^{1}H + {}^{1}H \rightarrow {}^{2}H + \beta^{+} + \nu$$
$$^{1}H + {}^{2}H \rightarrow {}^{3}He + \gamma$$
$$^{3}He + {}^{3}He \rightarrow {}^{4}He + {}^{1}H + {}^{1}H$$

where β^{+} is a positron, ν a neutrino, and γ a gamma ray, releasing about 26 MeV.

As the mass of the star increases, another sequence of reactions takes over to fuse H into He. Hans Bethe in 1938 proposed the "CNO cycle" of nucleosynthesis where ^{12}C acts as a catalyst to assemble four H atoms into one He atom [*Bethe*, 1939]. With the presence of a small amount of ^{12}C, the following sequence of reactions occurs:

$$^{12}C + {}^{1}H \rightarrow {}^{13}N + \gamma$$
$$^{13}N \rightarrow {}^{13}C + \beta + + \nu$$
$$^{13}C + {}^{1}H \rightarrow {}^{14}N + \gamma$$
$$^{14}N + {}^{1}H \rightarrow {}^{15}O + \gamma$$
$$^{15}O \rightarrow {}^{15}N + e^{+} + \nu$$
$$^{15}N + {}^{1}H \rightarrow {}^{12}C + {}^{4}He$$

This reaction path liberates about 25 MeV of energy, but occurs only over a narrow temperature range and hence is concentrated in the cores of high mass stars, whereas the proton–proton reactions can occur in portions of the star farther from its center. A variety of other nuclear reactions also occur with H under these stellar conditions, but the CNO cycle is the most efficient at transforming hydrogen into helium. While this process is occurring, any ^{14}N present also reacts with ^{4}He to form ^{18}O, which can capture another ^{4}He to form ^{22}Ne. Elements heavier than Ne are made only in very small quantities during the hydrogen-burning phase.

Once the hydrogen is consumed in the stellar core, without the energy of fusion, the star again begins to contract due to gravity. For stars with masses less than about half that of the Sun, gravity is not sufficient to compress the stellar core to the point of initiating fusion of heavier elements. The low-mass star simply shrinks in diameter and cools to become a red dwarf. For stars of about half to ten solar masses, the gravitational contraction after hydrogen exhaustion in the stellar core brings outer, still H-rich, portions of the star to pressures and temperatures where H-burning reactions can begin in a shell surrounding the core. The energy released from these reactions causes the luminosity of the star to increase greatly and drives the outer envelope of the star to expand, increasing the star's diameter greatly, but reducing its surface temperature. The combination of these effects leads the star to be called a Red Giant [Salaris *et al.*, 2002]. In this phase, core pressures and temperatures eventually reach the point where helium fusing reactions can begin, the most prominent of which is:

$$^{4}He + {}^{4}He + {}^{4}He \rightarrow {}^{12}C$$

As the ^{12}C concentration builds up, it can capture a ^{4}He nuclei to form ^{16}O, so that by the end of the core He-burning phase the star develops a core rich in C and particularly ^{16}O. At this point, He-burning moves out into the shell surrounding the core, with H-burning reactions still taking place in an outer layer in the star. This phase of stellar evolution is known as the Asymptotic Giant Branch, or AGB star [*Lattanzio and Forestini*, 1999]. At the end of the He-burning phase, temperatures and pressures are high enough to instigate the reaction:

$$^{13}C + {}^{4}He \rightarrow {}^{16}O + n$$

Reactions of this type are critical because they produce free neutrons (n) that can then be captured by any heavy nuclide present to create elements of increasingly heavy mass

[*Burbidge et al.*, 1957]. When He-burning moves into the shell surrounding the core, the fusion reactions can become unstable, resulting in brief bursts of intense He-burning, called helium shell flashes, that dramatically increase the luminosity of the star for short time periods—a few hundred years—and can instigate convection within the star that dredges up the higher atomic mass material from the deep interior into shallower levels in the star. The presence of these seed heavy nuclei in neutron-rich regions in the star then leads to neutron capture reactions that can create heavier and heavier elements. At this phase of Red Giant evolution, the outer regions of the star are sufficiently cool that solids can begin to condense at the stellar surface. The dust generated by this condensation is then driven away from the star by radiation pressure, and it carries along the surrounding gas with it, creating "winds" of the newly synthesized elements that return into interstellar space eventually to be incorporated into a new star when it forms.

In stars more massive than about ten solar masses, the extremely high temperatures and pressures in their interior result in widespread nuclear fusion and hence the rapid consumption of their nuclear fuel. The lighter elements are consumed quickly in the interior of a high mass star, but there is sufficient gravity to create conditions conducive to fusion of heavier elements. High mass stars thus develop a layered structure where H-burning is occurring in an outer shell, He-burning in a shell inside that, continuing through C, O, Ne, Mg and eventually Si fusing shells. The eventual product of this heavy element fusion is iron, but as we saw in Fig. 2.2, making any element heavier than iron consumes, rather than produces, energy. Without the energy from fusion, gravity again takes over and collapses the stellar core until it reaches nuclear densities, at which point it can shrink no further. As a result, contraction is stopped, and stopped so violently that the star is disrupted in a giant explosion known as a core-collapse supernova, flinging the contents of the star back into interstellar space, eventually to be incorporated into other stars [*Smartt*, 2009].

2.5.2 Making elements heavier than iron: *s-, r-, p*-process nucleosynthesis

The main H- and He-burning phases of relatively low mass stars (<10 times the mass of the Sun) primarily turn H into He and then He into carbon. Higher mass stars continue these fusion steps up to the point where Fe and Ni are produced, but fusion reactions cannot proceed past that point as they begin to consume, rather than liberate, nuclear energy, quenching the fusion process in the interior of the star as a result. Making elements heavier than Fe generally involves neutron addition to preexisting seed nuclei. How this process occurs, and the resulting isotopes produced, depends on the rate of neutron addition, which, in turn, depends on the neutron density in various stellar environments [*Burbidge et al.*, 1957; *Meyer*, 1994].

At the neutron densities characteristic of AGB stars, free neutrons are in low enough abundance that the time between collisions of neutrons with other nuclei is long enough that unstable nuclei produced by neutron capture have time to decay back to the valley of stability on the chart of the nuclides. For example, if there are ^{43}Ca nuclei present, addition of one neutron produces stable ^{44}Ca. If ^{44}Ca captures a neutron, it produces unstable ^{45}Ca. If no additional neutron arrives before the ^{45}Ca decays, then the ^{45}Ca decays to stable ^{45}Sc, which can eventually capture a neutron to form unstable ^{46}Sc, which decays to stable ^{46}Ti, and so on, moving the atom in stair-step fashion up Z and A along the center of the valley of nuclear stability. This slow neutron capture is given the name *s*-process nucleosynthesis [*Arlandini et al.*, 1999]. At higher neutron densities, neutrons can be added to seed nuclei so rapidly that very neutron-rich, unstable, isotopes are produced. When the neutron flux is eventually reduced, the unstable nuclei will β–decay back towards the valley of stable nuclei. This rapid addition of neutrons is known as *r*-process nucleosynthesis. While originally thought to occur in core-collapse supernovae, the relative dearth of *r*-process nuclides in the galaxy suggests that the *r*-process occurs in less common events than supernovae, perhaps as a result of the collision of two neutron stars. Neutron stars are the remnants of supernovae explosions whose densities are so high that they are composed almost entirely of neutrons.

The element Sm provides a good example of the different contribution of *s*- and *r*-process nucleosynthesis to element production (Fig. 2.15). Starting, for example, with ^{140}Ce, addition of a neutron creates unstable ^{141}Ce that β-decays to ^{141}Pr. Adding a neutron to ^{141}Pr creates unstable ^{142}Pr that β-decays to stable ^{142}Nd. Sequential addition of neutrons then creates stable ^{143}Nd, ^{144}Nd, ^{145}Nd, ^{146}Nd and eventually unstable ^{147}Nd that β-decays first to unstable ^{147}Pm and again to long-lived ^{147}Sm. Sequential addition of neutrons to ^{147}Sm will produce stable ^{148}Sm, ^{149}Sm, and ^{150}Sm, ending with unstable ^{151}Sm that will β-decay to stable ^{151}Eu. This is the path of *s*-process nucleosynthesis in this mass range.

The *r*-process, in contrast, adds neutrons so fast that β-decay of unstable nuclei cannot keep up, so neutron-rich isotopes are made, moving the seed isotope out horizontally on the chart of the nuclides (Fig. 2.15). When the neutron flux is reduced, these very neutron-rich isotopes will β–decay back towards the valley of stability. For example, ^{149}Nd, ^{151}Nd, and ^{152}Nd will β-decay through their unstable Pm isobars until they reach stable ^{149}Sm, ^{151}Eu, and ^{152}Sm, respectively. In contrast, ^{144}Sm, ^{148}Sm, and ^{150}Sm are blocked from production by β-decay from the neutron-rich side of the nuclear chart by stable ^{144}Nd, ^{148}Nd, and ^{150}Nd. Of the Sm isotopes, ^{148}Sm and ^{150}Sm are thus made primarily by the *s*-process, ^{147}Sm and ^{149}Sm are made by both *s*-process and *r*-process, and ^{152}Sm and ^{154}Sm are made primarily by *r*-process nucleosynthesis.

A small number of stable isotopes exist on the proton-rich side of the valley of stability, for example ^{144}Sm (Fig. 2.15), which is stable because of its magic number (82) of neutrons. This isotope of Sm cannot be made by the *s*-process because neutron addition to Nd, starting at ^{142}Nd, continues to ^{146}Nd then to ^{147}Sm.

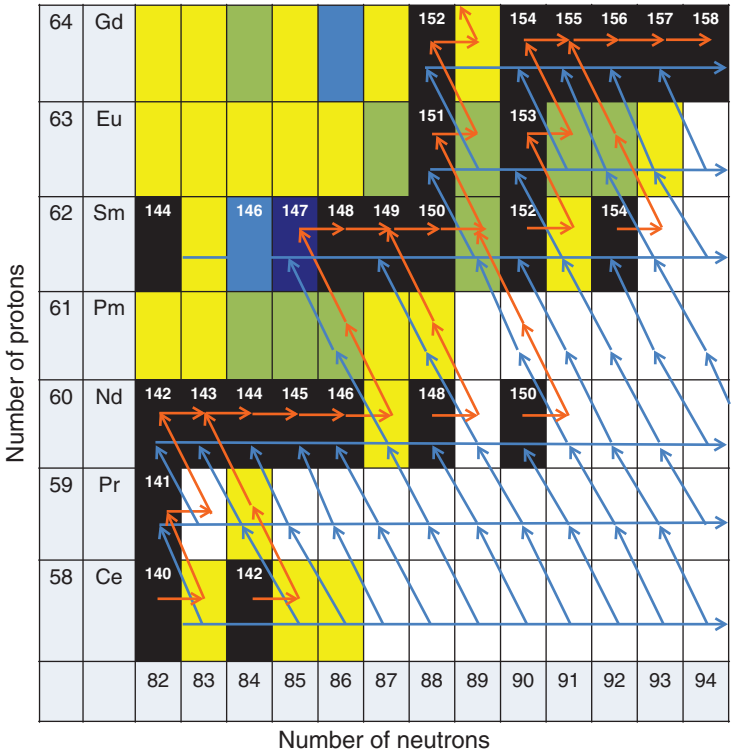

Fig. 2.15. Portion of the chart of the nuclides in the light rare earth element mass range showing the path of *s*- and *r*-process nucleosynthesis. The gray arrows show sequential neutron additions via the *s*-process followed by the β-decay that decreases *N*, and increases *Z*, by 1. The dark gray arrows show *r*-process nucleosynthetic paths that rapidly increase *N* creating a number of very neutron-rich isotopes that then β-decay back to stable isotopes. (*See insert for color representation of the figure*.)

Contributions of *r*-process nucleosynthesis to ^{144}Sm are blocked from the neutron-rich side of the nuclear chart by stable ^{144}Nd. Another synthesis mechanism thus must be sought for such proton-rich isotopes. Originally, these isotopes were believed to originate through proton capture by nuclei on the valley of stability, giving rise to the term *p*-process nucleosynthesis, but the efficiency of proton capture reactions is so low that this mechanism is unlikely to produce these isotopes in the quantity observed. Instead, proton-rich nuclei are most likely made by reactions that involve the absorption of either energetic gamma rays or neutrinos by a nuclear neutron that cause it to eject an electron and become a proton. Extremely high fluxes of both gamma rays and neutrinos are expected in the final stages of evolution of high mass stars on their way to supernova explosions, so *p*-process nucleosynthesis likely occurs in core-collapse supernovae, although the site of *p*-process nucleosynthesis remains uncertain.

2.5.3 Element abundances in the solar system

Both the stellar winds associated with AGB stars and the stellar disruption caused by supernova explosions hurl newly synthesized elements back into interstellar space. These elements eventually become incorporated into newly formed stars where the process of nucleosynthesis continues anew. While the lifetime of a low-mass star like the Sun may be as long as 10^{10} years, a high-mass star may last less than 10^7 years before it becomes a supernova. In a universe that is about 14 billion years old, the elemental composition of the galaxy and our own solar system reflects the elemental contributions from numerous stars and the likelihood that at least some fraction of the elements have been through more than one stellar nucleosynthetic cycle.

Figure 2.16 shows the element abundances in our solar system as deduced from measurements of the Sun's photosphere and from primitive meteorites [*Lodders*, 2003; *Palme and Jones*, 2003]. The shape of the abundance curve versus mass clearly reflects several aspects of nuclear stability. First, H and He are by far the most abundant elements in the solar system (note the log scale), reflecting the fact that element processing in stars still has a long way to go to reach the lowest nuclear energy state of a pure-iron universe. Elements of even-*Z* are more abundant than those with odd-*Z*, reflecting the additional stability created by nucleon paring. Carbon-12 and ^{16}O are particularly abundant, reflecting their end-product relationship in the He-burning phase of nucleosynthesis. Iron is unusually abundant amongst the

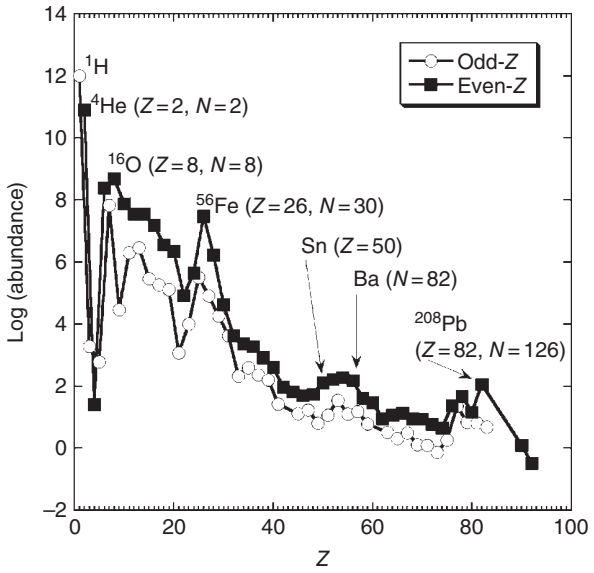

Fig. 2.16. Abundance of the elements in our solar system [*Lodders*, 2003]. Elements with an even number of protons (*Z*) are shown by filled squares, those with an odd number of protons are open circles.

heavy elements as a result of this nuclide having the highest binding energy per nucleon of any element. Element abundances decline rapidly from the iron peak with small peaks in abundance near the nuclear magic numbers of 50, 82 and neutron numbers of 126. The abundance peak at ^{208}Pb is particularly evident, as this isotope has filled nuclear shells of both protons (Z = 82) and neutrons (N = 126).

2.6 ORIGIN OF RADIOACTIVE ISOTOPES

2.6.1 Stellar contributions of naturally occurring radioactive isotopes

Besides the stable isotopes that constitute the elements in our solar system shown in Fig. 2.16, stellar nucleosynthesis also creates a vast array of radioactive isotopes. Some of these radioactive isotopes, for example ^{56}Ni (half-life of 6 days) decay so rapidly, and are so abundant, that they contribute substantially to the light output of the supernova in the days/weeks following the initial explosion. Others have long enough decay times that they survive transport through interstellar space and are incorporated into newly formed stars and planetary systems, such as our own. For those with long enough decay times, their abundance in the solar system likely reflects something of an average of all of the many stellar contributions to the region of the Milky Way from which the Sun formed. Their abundances are termed "galactic background," which nevertheless vary in different parts of the galaxy in proportion to the density of star forming regions, which, in turn reflects the mass present in a given portion of the galaxy (Fig. 2.17).

Table 2.1 lists the stellar-sourced radioactive isotopes that were present when our solar system formed. Those radioisotopes with half-lives on the shorter end of those listed in Table 2.1 may also include a contribution from the last stellar contribution to the solar nebula, enhancing their abundance over the galactic background.

2.6.2 Decay chains

The early work on radioactivity in uranium and thorium ores found that the ores contained several elements that had differing radioactive emissions, but the same chemical properties. Following this observation, T.W. Richards in 1914 reported that lead separated from uranium ores had a different atomic weight than did normal lead. With the eventual discovery of isotopes, these observations were transformed into the realization that U and Th undergo many different radioactive decays on their way to stable lead, creating a variety of elements along the way. The steps in the U and Th decay chains are summarized in Tables 2.2 through 2.4. These decay chains are unique amongst the stellar-produced radioactive isotopes where most transformations go from parent to daughter isotope in a single step. The U and Th decay chains produce a wide range of radioactive isotopes, some with half-lives long enough to be useful to track a variety of geologic processes as explored in Chapter 12.

2.6.3 Cosmogenic nuclides

As outlined in section 2.4, the extremely high pressure and temperature conditions in stellar interiors produce both nuclei and individual nucleons of sufficient energy to penetrate the Coulomb barrier of the nucleus, thus instigating nuclear reactions and creating new stable and radioactive isotopes. Outside of stars, nucleons with sufficient energy to cause nuclear reactions are found in cosmic rays, in the particles emitted by radioactive decay of other isotopes, and in man-made settings that include nuclear reactors, particle accelerators, and nuclear bombs.

Cosmic rays consist of very high energy nuclear particles, about 90% of which are single protons, 9% are α particles and 1% are nuclei of heavier elements [*Meyer*, 1969]. A small fraction of cosmic rays consist of high-energy β particles. One source of cosmic rays is the Sun. Solar cosmic rays, mostly protons (98%) and α particles, have energies generally within the range of 1–50 MeV. The flux of solar cosmic rays reaching Earth averages about 70,000 protons m^{-2} s^{-1}, but is variable throughout the 11-year solar cycle reflected in the periodic abundance of sunspots and solar flares.

Cosmic rays of much higher energy are known as galactic cosmic rays (GCR), with fluxes at 1 GeV energies of about 30,000 m^{-2} s^{-1} (Fig. 2.18) [*Amato*, 2014]. The sources of GCR are not entirely clear, but are definitely outside of the solar system, likely emitted by charged particle acceleration in the outflows of supernovae. Extremely high energy (> 10^{15} eV) GCR may originate from extragalactic sources, perhaps from active galactic nuclei

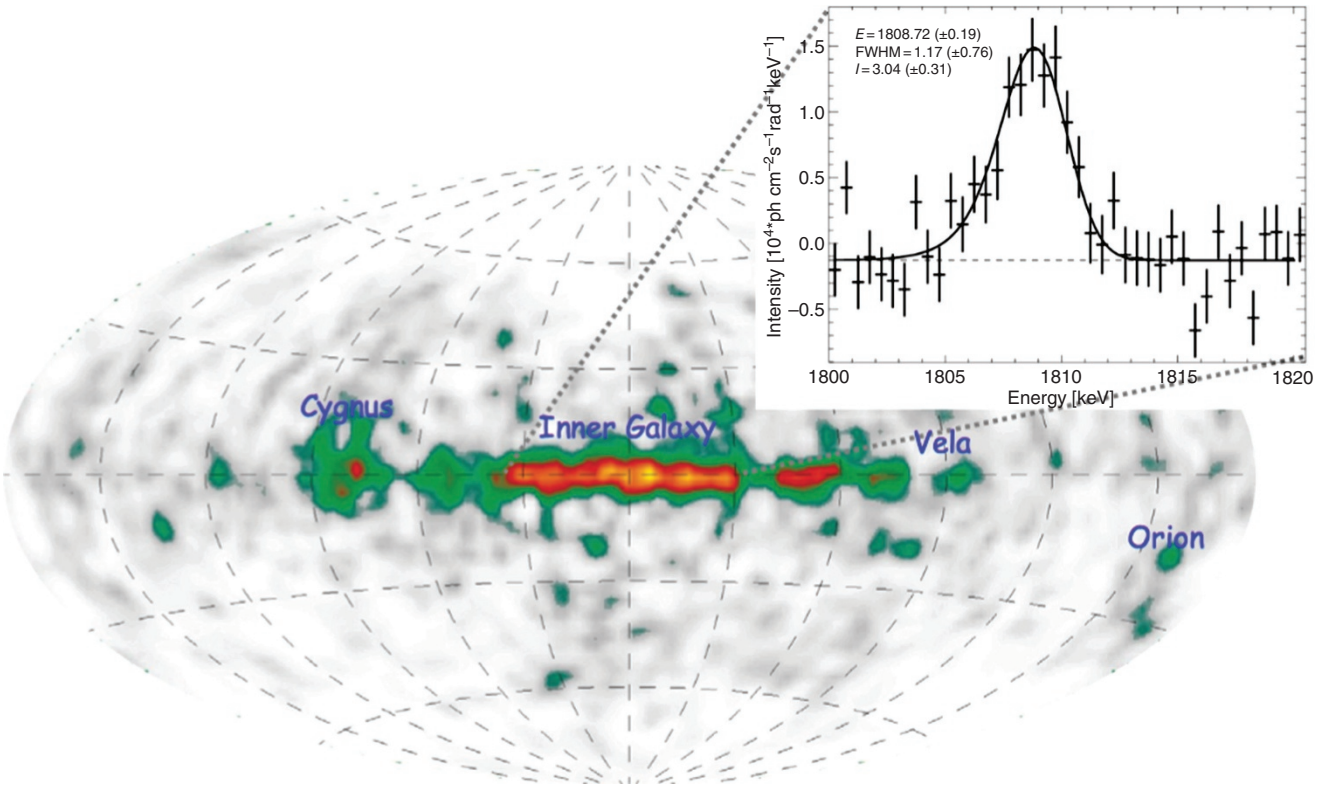

Fig. 2.17. COMPTEL map of ^{26}Al abundance and the INTEGRAL/SPI ^{26}Al gamma-ray spectrum from the inner Milky Way galaxy. Darker colors reflect the highest abundances of ^{26}Al near the galactic center and other areas of active star formation, with gray and white reflecting lower abundances at the outskirts of the galaxy. The graph in the upper left shows the distribution of gamma ray intensity versus energy. *E* shows the peak energy, FWHM is the "full-width, half-maximum" of the distribution of energy, and *I* is the standard deviation of the data. (Source: Courtesy of Roland Diehl.) (*See insert for color representation of the figure.*)

Table 2.1 Stellar-sourced radioactive isotopes

Parent isotope	Daughter isotope	Half-life (10^6 years)
^{26}Al	^{26}Mg	0.73
^{60}Fe	^{60}Ni	1.5
^{53}Mn	^{53}Cr	3.7
^{107}Pd	^{107}Ag	6.5
^{182}Hf	^{182}W	9
^{129}I	^{129}Xe	15.7
^{146}Sm	^{142}Nd	68
^{244}Pu	Fission Xe	80
^{235}U	^{207}Pb	704
^{40}K	^{40}Ar, ^{40}Ca	1270
^{238}U	^{206}Pb	4469
^{232}Th	^{208}Pb	14,010
^{176}Lu	^{176}Hf	37,100
^{187}Re	^{187}Os	41,600
^{87}Rb	^{87}Sr	49,500
^{147}Sm	^{143}Nd	106,000
^{190}Pt	^{186}Os	450,000

Table 2.2 ^{238}U decay chain

Parent	Decay mode	Half-life	Daughter
^{238}U	α	4.51×10^9 years	^{234}Th
^{234}Th	β	24.1 days	^{234}Pa
^{234}Pa	β	1.2 min, and 6.7 h	^{234}U
^{234}U	α	2.48×10^5 years	^{230}Th
^{230}Th	α	7.52×10^4 years	^{226}Ra
^{226}Ra	α	1622 years	^{222}Rn
^{222}Rn	α	3.82 days	^{218}Po
^{218}Po	α (99.98%), β	3.05 min	^{214}Pb, ^{218}At
^{218}At	α	1.3 s	^{214}Bi
^{214}Pb	β	26.8 min	^{214}Bi
^{214}Bi	β (99.96%), α	19.7 min	^{214}Po, ^{210}Tl
^{214}Po	α	10^{-4} s	^{210}Pb
^{210}Tl	β	1.32 min	^{210}Pb
^{210}Pb	β, α (10^{-6} %)	22 years	^{210}Bi, ^{206}Hg
^{210}Bi	β, α (5×10^{-5} %)	5 days	^{210}Po, ^{206}Tl
^{206}Hg	β	8.5 min	^{206}Tl
^{210}Po	α	138 days	^{206}Pb
^{206}Tl	β	4.3 min	^{206}Pb

that have central black holes with sufficient magnetic field strength to accelerate charged particles to such high energies. Their flux is more than 16 orders of magnitude lower than the peak GCR flux at ~300 MeV. The majority of solar cosmic rays are of insufficient energy to penetrate Earth's magnetic field. Galactic cosmic rays can penetrate Earth's magnetic field, but the majority of their primary particles interact with atoms in the upper atmosphere to make a cascade of secondary particles including protons, neutrons, and muons that can reach Earth's surface.

Table 2.3 ^{235}U decay chain

Parent	Decay Mode	Half-life	Daughter
^{235}U	α	7.13×10^8 years	^{231}Th
^{231}Th	β	25.6 h	^{231}Pa
^{231}Pa	α	3.48×10^4 years	^{227}Ac
^{227}Ac	β (98.8%), α	22 years	^{227}Th, ^{223}Fr
^{227}Th	α	18.2 days	^{223}Ra
^{223}Fr	β, α (4×10^{-3} %)	22 min	^{223}Ra, ^{219}At
^{223}Ra	α	11.7 days	^{219}Rn
^{219}At	α (97%), β	0.9 min	^{215}Bi, ^{219}Rn
^{219}Rn	α	3.9 s	^{215}Po
^{215}Bi	β	8 min	^{215}Po
^{215}Po	α, β (5×10^{-4} %)	0.0018 s	^{211}Pb, ^{215}At
^{211}Pb	β	36.1 min	^{211}Bi
^{215}At	α	0.0001 s	^{211}Bi
^{211}Bi	α (99.68%), β	2.15 min	^{207}Tl, ^{211}Po
^{207}Tl	β	4.8 min	^{207}Pb
^{211}Po	α	0.5 s	^{207}Pb

Table 2.4 ^{232}Th decay chain

Parent	Decay mode	Half-life	Daughter
^{232}Th	α	1.39×10^{10} years	^{228}Ra
^{228}Ra	β	6.7 years	^{228}Ac
^{228}Ac	β	6.1 h	^{228}Th
^{228}Th	α	1.9 years	^{224}Ra
^{224}Ra	α	3.6 days	^{220}Rn
^{220}Rn	α	54.5 s	^{216}Po
^{216}Po	α	0.16 s	^{212}Pb
^{212}Pb	β	10.6 h	^{212}Bi
^{212}Bi	β (66.3%), α	60.6 min	^{212}Po, ^{208}Tl
^{212}Po	α	3×10^{-7} s	^{208}Pb
^{208}Tl	β	3.1 min	^{208}Pb

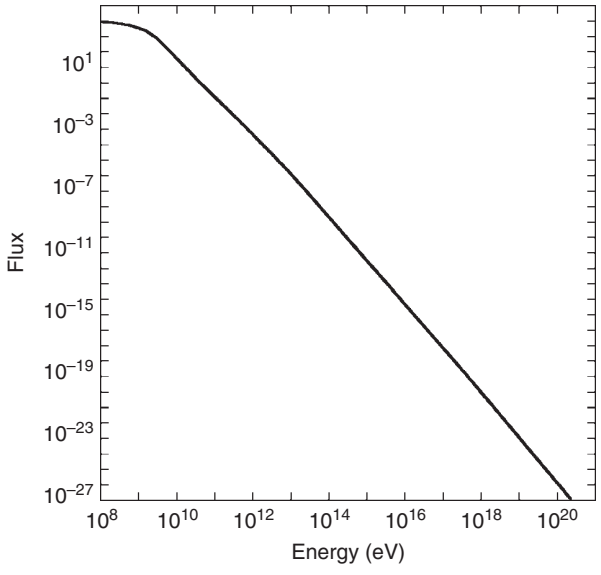

Fig. 2.18. Flux of cosmic rays versus energy. Flux is provided in units of particles per square meter per second. The lowest energy particles (<10^{10} eV)) are mostly solar cosmic rays, intermediate energy particles (10^{10} to 10^{15} eV) are galactic cosmic rays and the highest energy region is attributed to extragalactic cosmic rays. (Source: Lafebre, https://commons.wikimedia.org/wiki/File: Cosmic_ray_flux_versus_particle_energy.svg#. Used under CC BY-SA 3.0 https://creativecommons.org/licenses/by-sa/3.0/deed.en)

Table 2.5 Cosmic ray produced radioactive isotopes

Isotope	Decay mode[a]	Half-life	Daughter
^3H	β–	12.3 years	^3He
^3He		Stable	
^7Be	ec	53.3 days	^7Li
^{10}Be	β–	1.39×10^6 years	^{10}B
^{14}C	β–	5730 years	^{14}N
^{21}Ne		Stable	
^{22}Na	β+	2.6 years	^{22}Ne
^{26}Al	β+	730,000 years	^{26}Mg
^{32}Si	β–	101 years	^{32}P
^{32}P	β–	14.3 days	^{32}S
^{35}S	β–	87.5 days	^{35}Cl
^{36}Cl	β–	301,000 years	^{36}Ar
^{39}Ar	β–	269 years	^{39}K
^{41}Ca	ec	130,000 years	^{41}K
^{53}Mn	ec	3.8×10^6 years	^{53}Cr
^{60}Fe	β–	10^5 years	^{60}Ni
^{81}Kr	ec	210,000 years	^{81}Br
^{85}Kr	β–	10.7 years	^{85}Rb
^{129}I	β–	15.9×10^6 years	^{129}Xe

[a] β+ positron, β– electron, ec – electron capture.

With energies in the MeV range and beyond, cosmic rays can penetrate the Coulomb barrier of the nucleus, fragmenting the impacted nucleus in the process known as spallation. Spallation leads to production of a number of radioactive and stable nuclei that are either small fragments of the impacted nucleus (e.g., ^3He) or atoms with slightly lower atomic mass than the target nuclide. Another product of such violent collisions are free neutrons and muons. Muons are elementary particles similar to an electron that have a single negative charge, but a much larger mass of about 106 MeV. Both the neutrons and muons can then go on to additional reactions with the nuclei of nearby atoms. Primary target atoms for spallation by cosmic rays are N, O, Ar, and C in the atmosphere and C, O, Si, Mg, Al, and Fe in rocks. Table 2.5 provides a list of the most useful isotopes produced by cosmic ray interactions. Most of these isotopes are produced directly by spallation. The exceptions include ^{14}C that is produced by capture of a cosmic-ray-produced secondary neutron by ^{14}N, which emits a proton to become ^{14}C. Tritium (^3H) is produced when ^{14}N captures an energetic secondary neutron to split into ^{12}C and ^3H. Isotopes produced by interaction with cosmic rays are termed "cosmogenic" isotopes and can be either radioactive or stable isotopes. The many and varied applications of cosmogenically produced isotopes in geochronology are described in Chapter 13.

2.6.4 Nucleogenic isotopes

The α–decay of ^{147}Sm and particularly U, Th, and their decay-chain daughter isotopes produces α particles of sufficient energy to react with the nuclei of surrounding atoms. Isotopes produced through this route are termed "nucleogenic" [*Wetherill*, 1954]. The interaction of the α particles with surrounding atoms also can produce free neutrons, which can then go on to instigate additional nuclear transformations. Some important nucleogenic isotopes, and the reactions that produce them, include:

$^{6}Li + n \rightarrow {}^{3}H + \alpha$: ^{3}H then β^{-} decays to ^{3}He with a half-life of 12.3 years

$^{17}O + \alpha \rightarrow {}^{20}Ne + n$

$^{18}O + \alpha \rightarrow {}^{21}Ne + n$

$^{19}F + \alpha \rightarrow {}^{22}Na + n$: ^{22}Na then β^{+} decays to ^{22}Ne with a half-life of 2.6 years

$39K + n \rightarrow {}^{39}Ar + p$: ^{39}Ar then β^{-} decays back to ^{39}K with a half-life of 269 years

where n is a neutron, p a proton, and α an α particle. Another common way to write such reactions is, for example:

$^{39}K\,(n,p)^{39}Ar$

which signifies that neutron capture by ^{39}K will produce ^{39}Ar and a proton. Nucleogenic isotopes have not seen much use in geochronology, though recent attempts to use the (U–Th)/Ne system as a chronometer show promise [*Cox et al.*, 2015].

2.6.5 Man-made radioactive isotopes

By exploiting many of the same reaction paths described earlier in this chapter, particle accelerators, fission reactors, and nuclear bombs can produce a vast array of radioactive isotopes. For example, after the Fukushima Daiichi nuclear power plant was damaged by the tsunami generated by the 2011 Tohoku earthquake, a wide variety of fission-produced radionuclides were released into the environment. These included ^{90}Sr, ^{99}Tc, ^{129}Te, ^{131}I, ^{134}Cs, ^{136}Cs, ^{137}Cs, ^{140}Ba and ^{140}La. A general background level of ^{239}Pu and ^{240}Pu is found everywhere on Earth as a result of fallout from nuclear bomb testing in the 1950s and 1960s. Another product of atmospheric nuclear bomb testing was a big spike in the abundance of ^{14}C, in the amount of several tons, almost doubling the amount of ^{14}C in the atmosphere for a short time.

2.7 CONCLUSIONS

The properties of the nucleus allow us to address first-order questions ranging from the energy source of stars, the composition of the solar system, and the history of Earth. The production of radioactive isotopes in stars, radioactive decay chains, cosmic ray interactions, or nuclear reactors creates many isotopic clocks. The range in decay half-lives of these radioactive species provides chronological information over time periods from the age of the universe to the age of a human artifact. The availability of radioactive isotopes of elements with very diverse chemical behavior provides chronometers for a wide range of geochemical processes from igneous differentiation, volatile loss at a planetary scale, core formation, deposition of sediments, uplift of mountains or burial of sediments, mixing in the oceanic water column, the age of groundwater, as well as a vast array of applications in archeology and paleoecology. In the end, radioactive isotope geochronology provides the chronometer for Earth history. The remaining chapters in this book describe the many and varied ways in which radioactive isotopes can be used to decipher Earth history.

2.8 REFERENCES

Amato, E. (2014) The origin of galactic cosmic rays. *International Journal of Modern Physics: Conference Series* **1**. DOI: 10.1142/S0218271814300134.

Arlandini, C., Kappeler, F., Wisshak, K., *et al.* (1999) Neutron capture in low-mass asymptotic giant branch stars: cross sections and abundance signatures. *The Astrophysical Journal* **525**, 886–900.

Basdevant, J.-L., Rich, J., and Spiro, M. (2005) *Fundamentals in Nuclear Physics: From Nuclear Structure to Cosmology*. Springer, Berlin.

Bellini, G., Benziger, J., Bonetti, S., *et al.* (2010) Observation of geo-neutrinos. *Physics Letters* **B687**, 299–304.

Bethe, H. A. (1939) Energy production in stars. *Physical Review* **55**, 434–456.

Burbidge, E. M., Burbidge, G. R., Fowler, W. A., and Hoyle, F. (1957) Synthesis of the elements in stars. *Reviews of Modern Physics* **29**, 547–654.

Chadwick, J. (1932) Possible existence of a neutron. *Nature* **129**, 312.

Cox, S. E., Farley K. A., and Cherniak, D. J. (2015) Direct measurement of neon production rates by (α,n) reactions in minerals. *Geochimica et Cosmochimica Acta* **148**, 130–144.

Cross, W. G., Ing H., and Freedman, N. (1983) A short atlas of beta-ray spectra. *Physics in Medicine & Biology* **28**, 1251–1260.

Davis, E. A. and Falconer, I. J. (2005) *J.J. Thomson and the Discovery of the Electron*. Taylor & Francis, London.

Enge, W. (1980) Introduction to plastic nuclear track detectors. *Nuclear Tracks* **4**, 283–308.

Friedlander, G., Kennedy, J. W., Macias, E. S., and Miller, J. M. (1981) *Nuclear and Radiochemistry*. Wiley.

Irving, A. J., Kuehner, S., and Carlson R. W. (1997) 1.70 Ga Sm–Nd age for a garnet granulite xenolith from a minette sille, Sweetgrass Hills, Northern Montana supports Proterozoic collision of Hearne and Wyoming cratons. *EOS, Transactions of the American Geophysical Union* **78**, 786.

Krane, K. S. (1987) *Introductory Nuclear Physics*. Wiley.

L'Annunziata, M. F. (2007) *Radioactivity: Introduction and History*. Elsevier, Amsterdam.

Lattanzio, J. and Forestini, M. (1999) Nucleosynthesis in AGB stars. In *Asymptotic Giant Branch Stars*, Le Bertre, T., Lebre, A., and Waelkens, C. (eds). *Publications of the Astronomical Society of the Pacific* **111**, 125–126.

Lodders, K. (2003) Solar system abundances and condensation temperatures of the elements. *Astrophysical Journal* **591**, 1220–1247.

Mayer, M. G. (1950a) Nuclear configurations in the spin–orbit coupling model. I. Empirical evidence. *Physical Review* **78**, 16–21.

Mayer, M. G. (1950b) Nuclear configurations in the spin–orbit coupling model. II. Theoretical considerations. *Physical Review* **78**, 22–23.

Meshik, A. P. (2005) The workings of an ancient nuclear reactor. *Scientific American* **293**, 82–91.

Meyer, B. S. (1994) The *r*-, *s*- and *p*-process in nucleosynthesis. *Annual Review of Astronomy and Astrophysics* **32**, 153–190.

Meyer, P. (1969) Cosmic rays in the galaxy. *Annual Review of Astronomy and Astrophysics* **7**, 1–38.

Palme, H. and Jones, A. (2003) Solar system abundances of the elements. In *Treatise on Geochemistry*, Davis, A. M., (ed). Elsevier, Amsterdam.

Radash, L. (1968) Rutherford, Boltwood, and the age of the Earth: The origin of radioactive dating techniques. *Proceedings, American Philosophical Society* **112**, 157–169.

Reed, B. C. (2014) *The History and Science of the Manhatten Project*. Springer-Verlag, Berlin.

Rutherford, E. (1911) The scattering of alpha and beta rays by matter and the structure of the atom. *Philosophical Magazine* **6**, 21–47.

Salaris, M., Cassisi, S., and Weiss, A. (2002) Red giant branch stars: the theoretical framework. *Publications of the Astronomical Society of the Pacific* **114**, 375–402.

Smartt, S. J. (2009) Progenitors of core-collapse supernovae. *Annual Review of Astronomy and Astrophysics* **47**, 63–106.

Sramek, O., McDonough, W. F., Kite, E. S., Lekic, V., Dye, S. T., and Zhong, S. (2013) Geophysical and geochemical constraints on geoneutrino fluxes from Earth's mantle. *Earth and Planetary Science Letters* **361**, 356–366.

Stuewer, R. H. (1997) Gamow, alpha decay, and the liquid-drop model of the nucleus. *Astronomical Society of the Pacific Conference Series* **129**, 30–43.

Thomas, A. W. and Weise, W. (2001) *The Structure of the Nucleon*. Wiley.

Truran, J. W. J. and Heger, A. (2003) Origin of the elements. In: *Treatise on Geochemistry*, Davis, A. M., (ed). Elsevier, Amsterdam.

Wetherill, G. W. (1954) Variations in the isotopic abundances of neon and argon extracted from radioactive minerals. *Physical Review* **96**, 679–683.